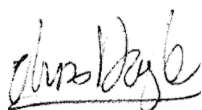


Customer : ESRIN	Document Ref : QA4EO-OQC-REP-VEG-5016
Contract No : 4000128960/19/I-NS	Issue Date : 10 October 2022
WP No : 1230	Issue : 1.0

Title : IDEAS-QA4EO – SMOS Monthly Report - September 2022

Abstract : This document provides a summary of the status and performance of SMOS over the course of the reporting month

Author :



IDEAS-QA4EO SMOS CEC
Team
QA4EO SMOS CEC Team

Accepted :

R. Crapolicchio on behalf of
ESA EOP-GMQ

Distribution :

Hard Copy File:

Filename: QA4EO-OQC-REP-VEG-5016_v1.0.docm

Copyright © 2022 Telespazio UK Ltd.

All rights reserved.

*No part of this work may be disclosed to any third party translated reproduced
copied or disseminated in any form or by any means except as defined in
the contract or with the written permission of Telespazio UK Ltd..*

Telespazio UK Ltd.

350 Capability Green, Luton, Bedfordshire, LU1 3LU, United Kingdom

Tel: +44 (0)1582 399 000 Fax: +44 (0)1582 728 686

www.vegaspacespace.com

TABLE OF CONTENTS

1	EXECUTIVE SUMMARY	5
2	INTRODUCTION.....	6
2.1	Structure of the Document	6
2.2	Reference Documents	6
2.3	Definitions of Terms	6
3	INSTRUMENT STATUS	9
3.1	Instrument Health	9
3.2	Instrument Unavailabilities and Anomalies	9
4	DATA SUMMARY.....	11
4.1	Reprocessing Activities	11
4.2	Operational Activities	11
4.3	Processing Changes	13
4.3.1	Processor Updates	13
4.3.2	Processor Status	13
4.3.3	Schema Updates	13
4.3.4	Schema Status	13
4.3.5	Auxiliary Files Updates	14
4.4	Calibration Events Summary.....	14
4.5	Data Coverage Summary.....	15
4.6	Summary of Degraded Data	16
4.7	Product Quality Disclaimers	16
5	LONG-TERM ANALYSIS	17
5.1	Calibration Analysis.....	17
5.2	Seasonal Evolution of the Calibration Parameters	17
5.3	Brightness Temperatures Trends over Dome-C Point (Antarctic)	29
5.4	Brightness Temperature Stability over the ocean:	31
5.5	L1C Quality Parameter Analysis	36
5.5.1	Software Errors.....	36
5.5.2	Instrument Errors	37
5.5.3	ADF Errors.....	39
5.5.4	Calibration Errors.....	40
5.5.5	Invalid Blocks.....	41
5.5.6	Discarded Scenes.....	42
5.6	L2OS Ocean Target Transformation (OTT) Orchestration Analysis	43
5.7	L2OS Retrievals Assessment	45
5.8	L2SM Retrievals Assessment	48
5.9	Pi-MEP: SSS Time series with Argo Buoys.	53
6	PRODUCT QUALITY ANALYSIS	56
7	ADF CONFIGURATION AT THE END OF THE REPORTING PERIOD	57
8	APPENDIX A. CONFIGURATION DOCUMENT LIST	60

AMENDMENT POLICY

This document shall be amended by releasing a new edition of the document in its entirety. The Amendment Record Sheet below records the history and issue status of this document.

AMENDMENT RECORD SHEET

ISSUE	DATE	DCI No	REASON
1.0	10/10/2022	N/A	Formal release

This Page is Intentionally Blank

1 EXECUTIVE SUMMARY

This is the routine Soil Moisture and Ocean Salinity (**SMOS**) Monthly Public Report containing a summary of the instrument health, product quality status and updates to SMOS processing and auxiliary files during September 2022.

The instrument health during September 2022 was found to be nominal. There were five unavailabilities reported during the reporting period which translated into time intervals with data loss or degraded data. The list of unavailabilities is included in section 3.2.

The data quality during September 2022 was found to be nominal, with the exceptions listed in section 4.5. These degraded periods have been induced either by instrument anomalies or by unavailability of dynamic auxiliary files.

2 INTRODUCTION

2.1 Structure of the Document

After this introduction, the document is divided into several major sections that are briefly described below:

1 Executive summary

The executive summary covers the main findings from the report.

2 Introduction

A list of referenced documents and definitions of terms are available.

3 Instrument status

This section covers the instrument health and unavailabilities from this reporting period.

4 Data Summary

This section covers reprocessing, updates to processors and aux files as well as a data coverage summary.

5 Long Term Analysis

Long-term analysis of the instrument calibration and data quality are provided in this section.

2.2 Reference Documents

RD1	XSMS-GSEG-EOPG-TN-08-0016 SMOS L1OP-V3 Product Quality Flag format definition V3.1
-----	--

2.3 Definitions of Terms

The following terms have been used in this report with the meanings shown.

Term	Definition
CCU	Correlator and Control unit, instrument computer on-board
CMN	Control and Monitoring Node, responsible for commanding the receivers, reading their physical temperatures and telemetry and the generation of the synchronization signal (local oscillator tone) among receivers.
DPGS	Data Processing Ground Segment
ESL	Expert Science Laboratory
IC4EC	Internal Calibration for External calibration. Calibration sequences for the instrument monitoring and calibration of science data acquired in external target pointing.
IFREMER	French Research Institute for Sea Exploitation (Institut Français de Recherche pour l'Exploitation de la MER)

IPF	Instrument Processor Facility
L2OS	Level 2 Ocean Salinity
L2SM	Level 2 Soil Moisture
LICEF	Lightweight Cost Effective Receivers
MIRAS	Microwave Imaging Radiometer using Aperture Synthesis
MM	Mass Memory
N/A	Not applicable
OCM	Orbit Correction Manoeuvre
Pi-MEP	SMOS Pilot-Mission Exploitation Platform project
PMS	Power Measurement System
RFI	Radio Frequency Interference
SPQC	Systematic Product Quality Control facility
SSS	Sea Surface Salinity

This Page is Intentionally Blank

3 INSTRUMENT STATUS

3.1 Instrument Health

The current instrument status is that all the **instrument** subsystems are working correctly. The current configuration of the instrument is that the arm A and the arm B are working in nominal side and arm C is in the redundant side.

Table 3-1 History of instrument problems and mode changes

Start	Stop	Description
11 January 2010 12:07z Orbit 1013	N/A	Arm A changes from redundant to nominal side. That operation is to avoid the malfunction of one of the redundant CMNs of the arm.
12 January 2011 09:15z Orbit 6278	N/A	Arm B changes from redundant to nominal side. That operation is to avoid the malfunction of one of the redundant CMNs of the arm.

3.2 Instrument Unavailabilities and Anomalies

The unavailabilities and anomalies listed in Table 3-2 occurred during the reporting period. A full list of unavailabilities can be found in the Mission Status section on the SMOS Earthnet website accessible [here](#)

During these unavailabilities and anomalies the instrument may have either not collected data or may have collected corrupt data which may not have been processed to higher levels. Table 4-7, Table 4-8 and Table 4-9 provide details of the data which has been affected by gaps and quality degradation respectively.

Table 3-2 SMOS unavailability list

Start Time (UTC)	Stop Time (UTC)	Unavailability Report Reference	Planned	Description
03/09/2022 09:55:26z	03/09/2022 11:41:49z	FOS-5439	No	Memory Latch-up, partition P3
05/09/2022 05:38:31z	05/09/2022 05:42:10z	FOS-5445	No	CCU Reset
13/09/2022 02:15:51z	13/09/2022 02:25:51z	FOS-5455	No	CMN unlock on B3
18/09/2022 22:26:03z	18/09/2022 22:45:37z	FOS-5457	Yes	OCM

Start Time (UTC)	Stop Time (UTC)	Unavailability Report Reference	Planned	Description
26/09/2022 08:28:18z	26/09/2022 08:28:18z	FOS-5473	No	MM Latch up on partition P5

4 DATA SUMMARY

4.1 Reprocessing Activities

The information regarding to data reprocessing activities (REPR data type) is shown in the table below.

Table 4-1 Data Summary - REPR

Data type	Sensing start	Sensing stop	Version	Comments
L2	09/10/2019 17:40:46z	10/10/2019 19:35:05z	V700	ECMWF corrupted files affected the Reprocessing Campaign L2 data for that period. Data have been regenerated once the correct ECMWF dataset was available.
L2	31/03/2020	31/01/2021	V700	L2 V700 Reprocessing Catch-Up Campaign started on March 8 th 2021 and finished on March 27 th 2021.
L1	31/03/2020	31/01/2021	V724	L1 V724 Reprocessing Catch-Up Campaign began on March 8 th 2021 and finished on March 27 th 2021.
L2	13/04/2010	31/03/2020	V700	L2 V700 Full Reprocessing Campaign started on December 5 th 2020, and finished on March 4 th 2021.
L1	01/10/2019	31/03/2020	V724	L1 V724 Reprocessing Catch-Up Campaign began on May 22 nd 2020 and finished on May 29 th 2020.
L1	01/01/2010	30/09/2019	V724	L1 V724 Reprocessing Campaign began on January 2 nd 2020, finished on February 12 th 2020. Reprocessing of pending products finished on February 19 th 2020, concluding this reprocessing activity.

4.2 Operational Activities

The information regarding to the data regeneration activities (OPER data type) is shown in the table below:

Table 4-2 Data Summary - OPER

Reporting period			
Data type	Sensing start	Sensing stop	Comments
N/A	N/A	N/A	N/A
Previous reporting periods			
Data type	Sensing start	Sensing stop	Comments

L1 and L2 Science	29/06/2022 06:29:10z	29/06/2022 08:23:23z	Incomplete passes acquired in Svalbard. Data were re-covered with the next pass and reprocessed.
L1 and L2 Science	31/03/2022 00:52:55z	01/04/2022 11:57:47z	VTEC_P files arrived with delay creating degraded science data due to ADF errors. Period was regenerated once the corresponding VTEC_P files were made available.
L2OS	29/01/2022 12:07:50z	01/02/2022 21:04:44z	L2OS data between 28 th and 1 st of February lack retrievals for some areas. This had to do with L1C data flagged with instrument errors due to antenna temperature slightly higher than 29°C. Deeper analysis on this was carried out and it was agreed to reprocess the data and force the L2OS to retrieve the measurements, since no clear degradation is detected despite the surpassed of the temperature thresholds.
MIR_CSTD1A	16/12/2021 13:16:29z	17/12/2021 08:21:28z	Svalbard tracking issues on the 16th of December lead to incorrect orchestration of MIR_CSTD1A files. These data were successfully regenerated.
L1 and L2 Science	16/12/2021 11:29:43z	17/12/2021 14:53:52z	Svalbard tracking issues on the 16th of December lead to incorrect orchestration of MIR_CSTD1A files and degraded L1 and L2 science data. These data were successfully regenerated with no degradation.
L1 and L2 Science	06/11/2021 19:57:42z	06/11/2021 22:31:49z	Degraded L0 calibration due to acquisition pass affected by RFI in Svalbard. This led to degraded science data, period was successfully regenerated.
MIR_CSTD1A	06/11/2021 20:59:51z	07/11/2021 15:09:52z	L0 calibration degraded due to acquisition pass affected by RFI in Svalbard. These data were successfully regenerated.
Telemetry	06/11/2021 20:37:35z	06/11/2021 21:41:46z	Degraded TLM due to acquisition pass affected by RFI in Svalbard. These data were recovered in the next pass and successfully regenerated.
L1 and L2 Science	03/10/2021 23:41:28z	04/10/2021 02:15:33z	L0 calibration gap due to acquisition pass affected by RFI in Svalbard. This led to degraded science data, period was successfully regenerated.
MIR_CSTD1A	04/10/2021 00:41:39z	04/10/2021 19:41:40z	L0 calibration gap due to acquisition pass affected by RFI in Svalbard. These data were successfully regenerated.
Calibration	19/09/2021 01:08:55	19/09/2021 02:48:54	DPGS issues on the 19 th September 2021 led to a LO calibration gap in between 2021-09-19T01:08:55z and 2021-09-19T02:48:54z. The data has now been re-generated.
L2	15/06/2021 01:42:22z	17/06/2021 05:27:55z	Reprocessed period due to incorrect LSMASK orchestrated in the DPGS.
L1	15/06/2021 01:42:22z	17/06/2021 05:27:55z	Reprocessed period due to incorrect LSMASK orchestrated in the DPGS.

The information regarding the past version V5xx data regeneration and reprocessing activities (OPER and REPR data type) are available in the monthly report of April 2015.

The information regarding the past version v6xx data regeneration and reprocessing activities (OPER and REPR data type) are available in the monthly report of May 2021.

4.3 Processing Changes

4.3.1 Processor Updates

During the reporting period, no new processor versions were deployed into operations.

4.3.2 Processor Status

At the end of the reporting period, the Processing Facility is using the following processors:

Table 4-3 Instrument Processors status

Processor	Version	Deployment date
L1OP	724	25/05/2021
L2OS	700	25/05/2021
L2SM	700	25/05/2021

Table 4-4 Pre- and Post-processors status

Processor	Version	Deployment date
ECMWFP	318	07/11/2013
VTECGN	320	18/05/2016
OSCOTT	700	25/05/2021
L2 Post-processors	600	25/05/2021
SNOWP	102	28/10/2016

4.3.3 Schema Updates

No updates for product schema in the reporting period.

4.3.4 Schema Status

At the end of the reporting period, the schema version of the data block of the products generated and distributed through SMOS dissemination service is:

Table 4-5 Schema version status

Product type	Version
MIR_SC_F1B	402
MIR_SCSF1C	401
MIR_SCLF1C	401
MIR_BWSF1C	400
MIR_BWLF1C	400

Product type	Version
MIR_SMUDP2	400
MIR_OSUDP2	401
AUX_ECMWF_	300

The schema package v07.08.01, the XML Read/Write API libraries to read SMOS products, visualization and mapping tools for SMOS L1 and L2 products are available [here](#) (See [GMT](#) for the schemas)

Further information about the product format is available in the level 1 and level 2 product specification documents available [here](#)

4.3.5 Auxiliary Files Updates

The following quasi-static and dynamic AUX files were disseminated to the processing stations this reporting period. The status of the quasi-static and dynamic AUX files at the end of the reporting period is in the section 7.

- **AUX_BULL_B**

Note that, as reported in SPCM37, the format of the BULL_B primitive has been manually modified to obtain a properly formatted SMOS file. This is due to a small format change since February 2019 Bulletin B.

SM_OPER_AUX_BULL_B_20220702T000000_20220801T235959_120_001_3

Start sensing time at L1 processor: N/A

Justification: Bulletin Update including values from July 2022 and the prediction for August 2022. Its usage is intended for reprocessing.

SM_OPER_AUX_BULL_B_20220702T000000_20500101T000000_120_001_3

Start sensing time at L1 processor: 2022-09-16 06:14:06z

Justification: Bulletin Update including values from July 2022 and the prediction for August 2022. Its usage is intended for the nominal production.

4.4 Calibration Events Summary

The following table summarizes the major calibration activities conducted during the reporting period. The Local Oscillator calibration is not included in the table since occurs periodically every 10 minutes. The short calibrations are acquired weekly since 2011-03-24 and they are currently used in the nominal processing chain.

Table 4-6 Calibration summary

Date	Start Time	Stop Time	Calibration	Comments
01/09/2022	07:39:30z	07:41:14z	Short	Nominal
08/09/2022	06:27:00z	06:28:44z	Short	Nominal

Date	Start Time	Stop Time	Calibration	Comments
14/09/2022	15:30:49z	16:53:02z	Warm-NIR	Nominal Brightness Temperature 3.8519 K RMS: 0.5727 K Moon Elevation: 22.9817 Sun Elevation: 4.002543 Right Ascension (deg): 88.53 Declination (deg): -31.97
15/09/2022	06:54:30z	06:56:14z	Short	Nominal
22/09/2022	05:42:00z	05:53:44z	Short	Nominal
28/09/2022	14:43:01z	16:05:14z	Warm-NIR	Nominal Brightness Temperature 3.9471 K RMS: 0.7379 K Moon Elevation: -6.7355 Sun Elevation: 9.134150 Right Ascension (deg): 104.69 Declination (deg): -41.69
29/09/2022	06:09:30z	06:11:14z	Short	Nominal

4.5 Data Coverage Summary

Where instrument unavailabilities or anomalies have occurred during this reporting period, gaps in data coverage may have also occurred. A list of the gaps due to a permanent data loss is given in Table 4-7 by product level. On the other hand, a list of gaps due to operational problems is given in Table 4-8. The latter gaps may be recovered when the problem is fixed.

The science data gaps due to the execution of calibration activities are not listed in this section.

Table 4-7 Data loss summary

Start	Finish	Data Level	Comments
03/09/2022 09:55:26z	03/09/2022 11:41:49z	All	Memory Latch-up, partition P3 (FOS 4539)
05/09/2022 05:38:31z	05/09/2022 05:42:10z	All	CCU Reset (FOS-5445)
18/09/2022 22:26:03z	18/09/2022 22:45:37z	All	OCM (FOS-5457)

1: Data acquired during the manoeuvre is flagged as external pointing and not available as nominal data.

Table 4-8 Operational gaps summary

Start	Finish	Data Level	Comments
N/A	N/A	N/A	N/A

4.6 Summary of Degraded Data

In September 2022, SMOS data was affected by the following instrument and processing anomalies which have had a detrimental effect on the data quality.

Table 4-9 Summary of degraded data

Start	Finish	Affected products	Problem Description
13/09/2022 02:15:51z	13/09/2022 02:25:51z	L1a and above products	CMN unlock on B3 (FOS-5455)

4.7 Product Quality Disclaimers

The following product disclaimers affects the data generated in the reporting period:

Table 4-10 Summary of product quality disclaimers

Date	Product level	
From 28 th January 2022 To 02 nd February 2022	CSTD1A, L1C	Most CSTD1A and L1C products are flagged as Warning due to Instrument Error. This is related with the expected temperature increase of segment A1 during the eclipse season which has reached and slightly surpassed the threshold of 29°C used to set the flag. Temperature evolution of this LICEF is being monitored.
From: 12th January 2010 To: 1st August 2021	L1B	Direct_Sun_Correction_Type inside MIR_SC_F1B headers is incorrectly defined. Its value should be 4, which relates to "Correction by Measurements. BT Self-estimation with improved Sun Position Estimate Technique"
From: 21 st June 2017 (06:05:53z) To: 21 st June 2017 (07:28:07z)	L1	Due to CCU reset side effect science data was acquired with instrument pointing in external target looking at deep sky.

5 LONG-TERM ANALYSIS

5.1 Calibration Analysis

Since Level 1 product version v724, the dataset is processed with a fixed NIR noise temperature set to +424.41 [K] for H-Pol and +416.12 [K] for V-Pol. The impact is a more long-term stable Brightness Temperature measurements. The NIR calibration is performed only for monitoring purpose and results are presented in this section.

During the reporting period, there have been two Warm-NIR calibration events: the 14th and 28th of September.

The evolution of the noise temperature of the reference noise diodes T_{na} and T_{nr} computed with processor baseline V724 since March 2011 is shown from Figure 1 to Figure 4. The evolution of the NIR noise temperature parameters, which are related to the internal diode stability, are stable in particular for the NIR-CA. The small deviations in the NIR T_{na} calibration are due to either Radio Frequency Interference (RFI) that corrupted the calibration measurement (e.g. 3rd June 2015, 2nd August 2017), or HOT-NIR calibration with different thermal environment with the Sun above the antenna plane (e.g. 1st November 2020, 27th October 2021 and 22nd December 2021).

Currently, the calibration team is monitoring an ongoing evolution for the NIR CA T_{na} H-Pol which began end 2019. The origin of this evolution could be either internal reference diode power evolution or inaccuracy in the antenna losses thermal compensation during calibration. With reduced magnitude the effect is also present for the NIR CA T_{na} V-Pol.

5.2 Seasonal Evolution of the Calibration Parameters

The T_{na} and T_{nr} present in the previous processor baseline V5xx (see for example the monthly report for April 2015) had been largely mitigated by the new calibration algorithm, which decouples the variation of the antenna losses and the drift of the reference diode. This approach allows compensating each drift separately improving the diode stability monitoring and increasing the accuracy of the consequent calibration correction. Further improvements in the calibration stability were achieved by implementing the "Warm-NIR calibration" since 15th of October 2014. During "Warm-NIR calibration", the Noise Injection Radiometer (NIR) calibration is performed with a Sun elevation of 10 degrees above the antenna plane to maintain a stable thermal environment of the instrument through the calibration sequence.

Figure 5 and Figure 6 present the evolution of the NIR Observed Brightness Temperature (BT) since the beginning of the mission for V724 baseline. The small variation of a few Kelvins, in the observed BT are due to slightly different regions of the Sky sensed during the calibration manoeuvre. This parameter is used only for monitoring purpose.

The leakage and cross-coupling factors of the NIR channels shown in Figure 7 and Figure 8 remain small and no problems can be observed apart from a peak in the phase of the NIR-AB cross-coupling term on 11 April 2012. That peak corresponds to an anomaly in the NIR-AB that did not have impact on the data.

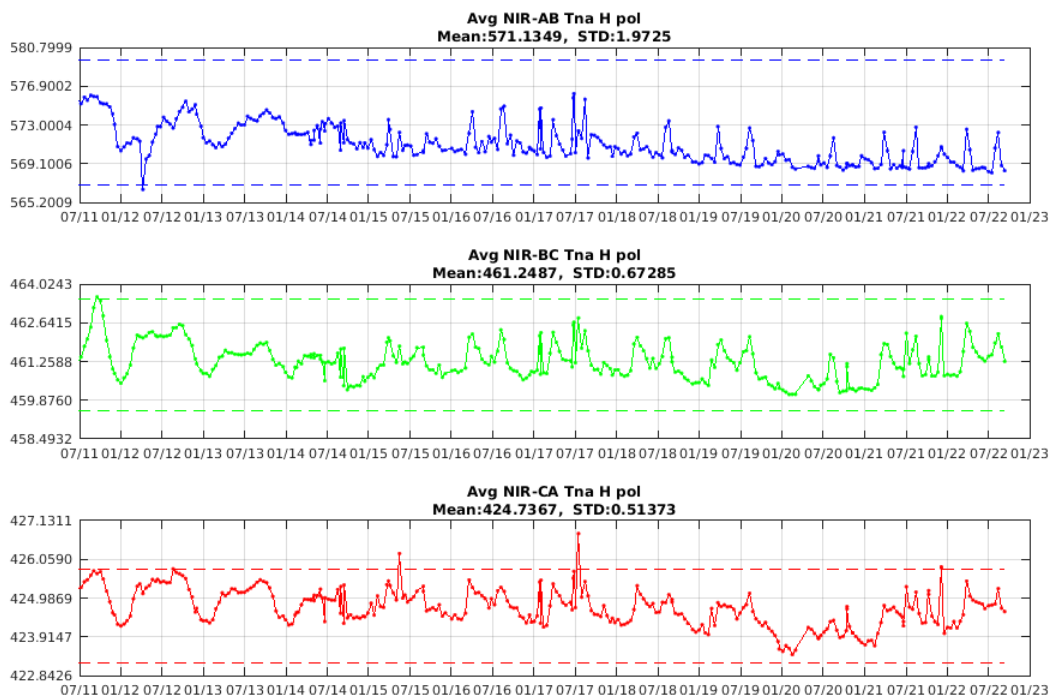


Figure 1 Tna evolution of NIR AB (blue), NIR BC (green) and NIR CA (red) in the H-channel since the beginning of the mission. Thresholds in dashed lines

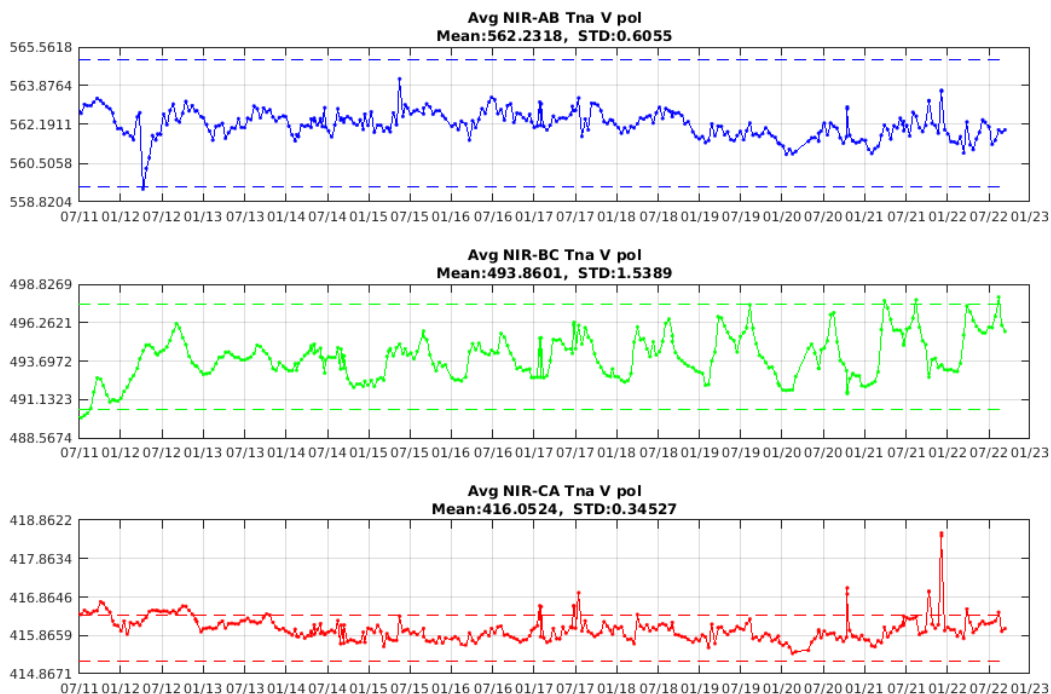


Figure 2 Tna evolution of NIR AB (blue), NIR BC (green) and NIR CA (red) in the V-channel since the beginning of the mission. Thresholds in dashed lines

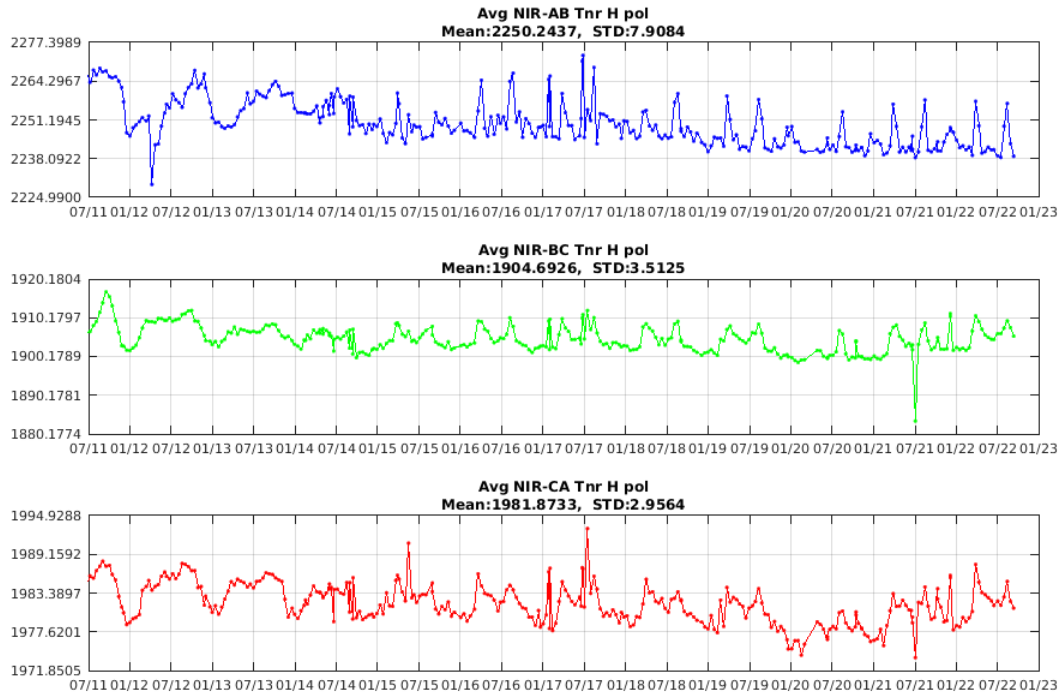


Figure 3 Tnr evolution of NIR AB (blue), NIR BC (green) and NIR CA (red) in the H-channel since the beginning of the mission.

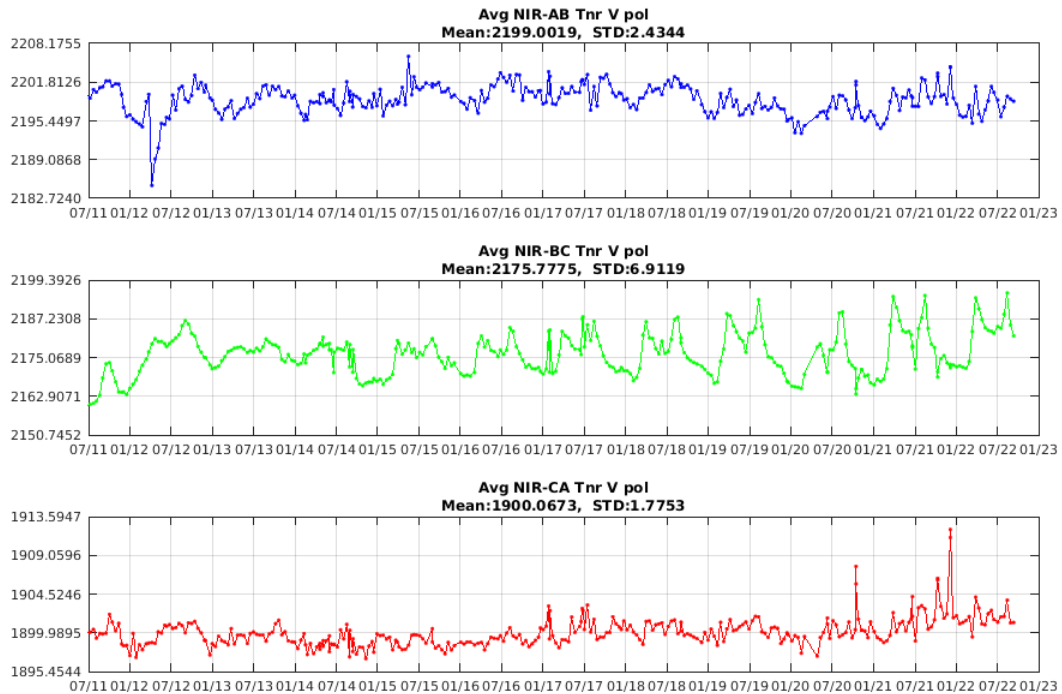


Figure 4 Tnr evolution of NIR AB (blue), NIR BC (green) and NIR CA (red) in the V-channel since the beginning of the mission.

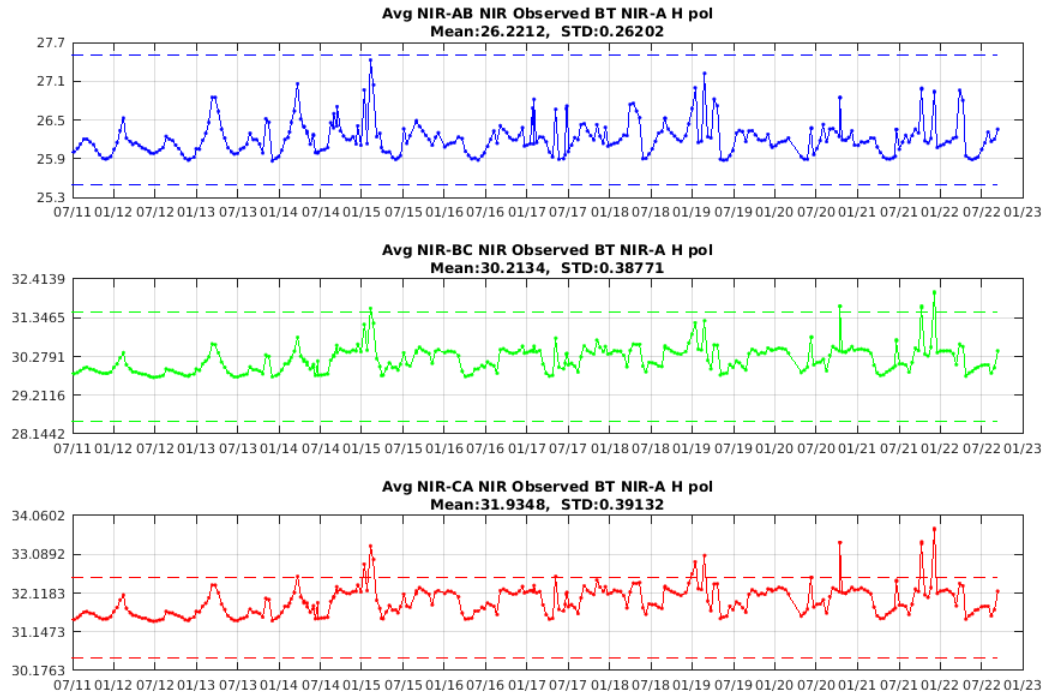


Figure 5 NIR Observed BT evolution of NIR AB (blue), NIR BC (green) and NIR CA (red) in the H-channel since the beginning of the mission. Thresholds in dashed lines

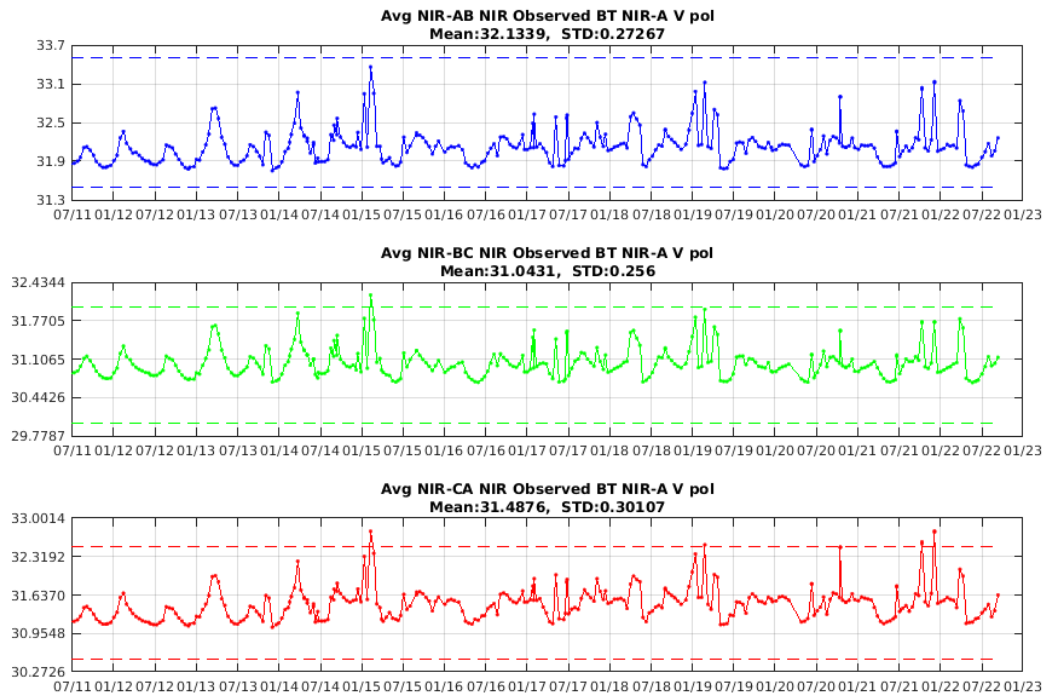


Figure 6 NIR Observed BT evolution of NIR AB (blue), NIR BC (green) and NIR CA (red) in the V-channel since the beginning of the mission. Thresholds in dashed lines

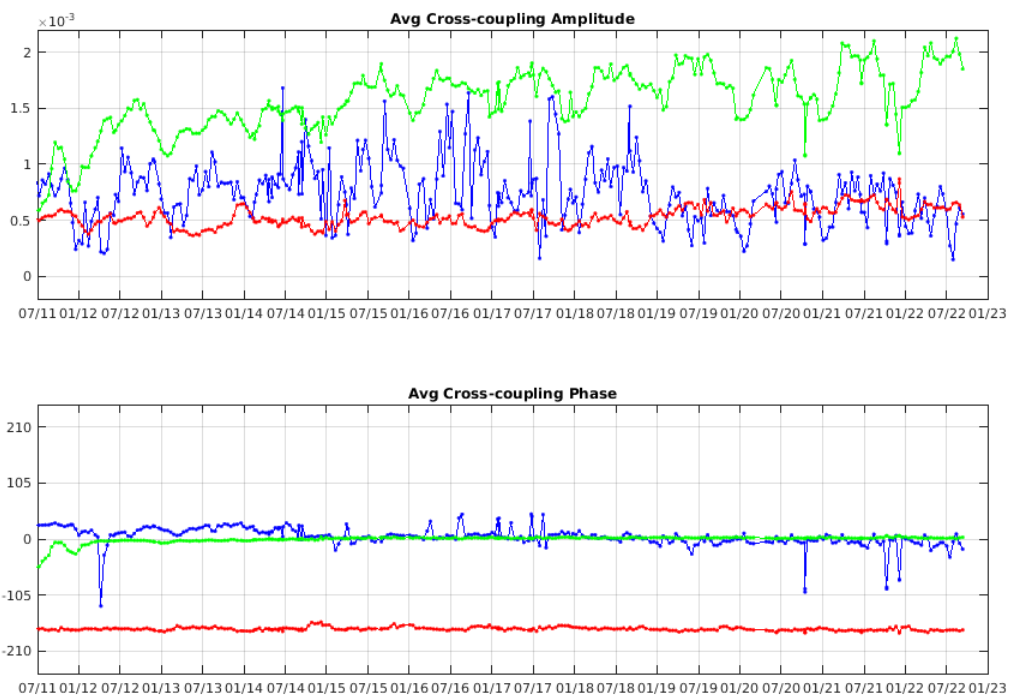


Figure 7 Cross-coupling evolution in amplitude and phase of NIR AB (blue), NIR BC (green) and NIR CA (red) since the beginning of the mission

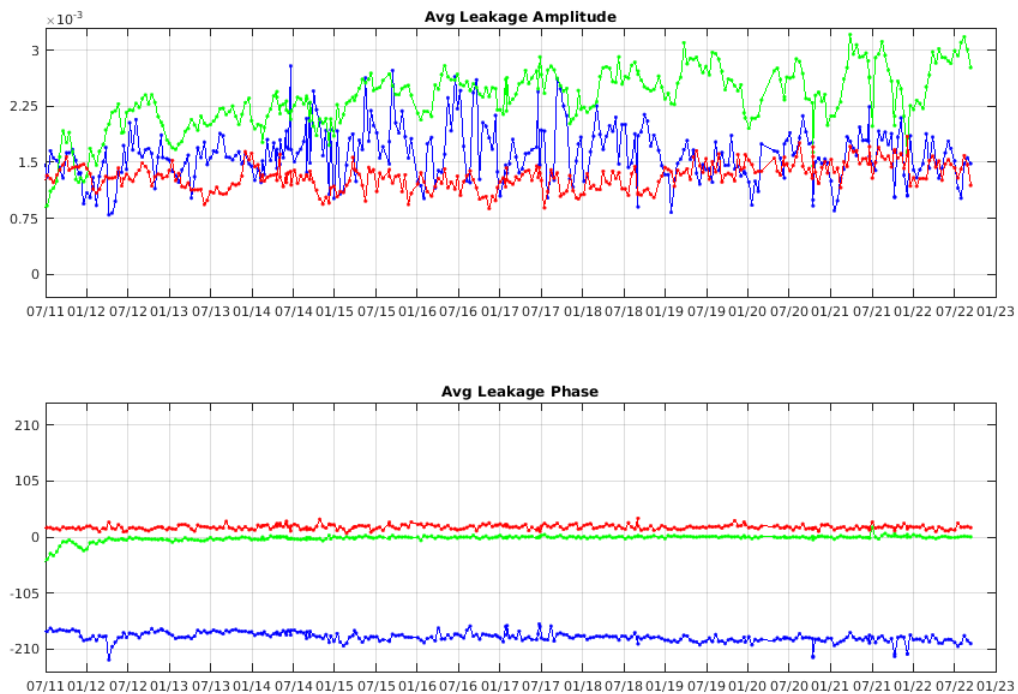


Figure 8 Leakage factor evolution in amplitude and phase of NIR AB (blue), NIR BC (green) and NIR CA (red) since the beginning of the mission

LICEFs

The Lightweight Cost Effective Receivers (LICEF) calibration status is updated by long (every 8 weeks) and short (weekly) on-board calibration activities. No long calibration was executed during the reporting period.

LICEF PMS gain is derived during the long calibration activity and Figure 9 to Figure 20 show the evolution (V724 algorithm baseline) of the deviations of the PMS gain with respect to its average over time. Note that PMS gain depends on the physical temperature of the receivers; PMS calibration is performed at slightly different physical temperature due to calibration time (season effect) and position of the receiver (LICEF) in the instrument (arms and central hub). To compare the calibration results the gains and offsets obtained during the calibration are normalised to 21 degrees Celsius temperature by using the receiver PMS gain and offset temperature sensitivity parameter (one value for each LICEF).

Apart from receiver (LICEF) LCF_A_18, LCF_C_11, LCF_C_19, which have shown a clear evolution from the main trend (see Figure 12, 19, 20) the others PMS gains are stable. The seasonal PMS gain variation present in some LICEFs for previous product version 6 has been mitigated in the current product version 7 by a better characterization of the PMS gain temperature sensitivity parameters. Few LICEFs still present seasonal PMS variation which needs further refinement for the sensitivity parameter.

Figures from Figure 21 to Figure 32 show the evolution of the PMS offsets (V724 algorithm baseline) derived during the short calibration activity.

Figure 33 shows the evolution of the average overall the baselines of the Fringe Washing Function (FWF) amplitude in the origin derived during the long calibration. The amplitude of the FWF at the origin shows a small drift since the beginning of the mission, nevertheless the values are inside the ranges defined in the routine calibration plan.

The evolution of the visibility average offsets (Figure 34 and Figure 35) had an unexpected peak on the 2nd of February 2017. According to preliminary analysis, this seems related to RFI. The quality impact on the data is small with a peak-to-peak bias of about 0.1K in brightness temperature.

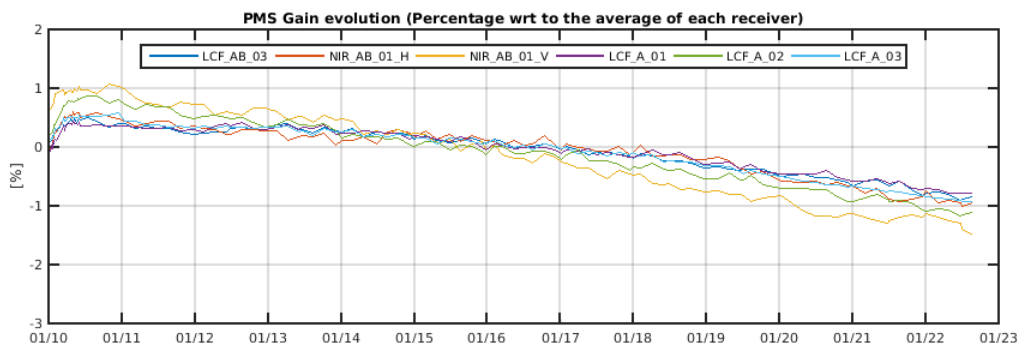


Figure 9 Evolution of the Δ PMS Gain of the LICEFS in CMN H1

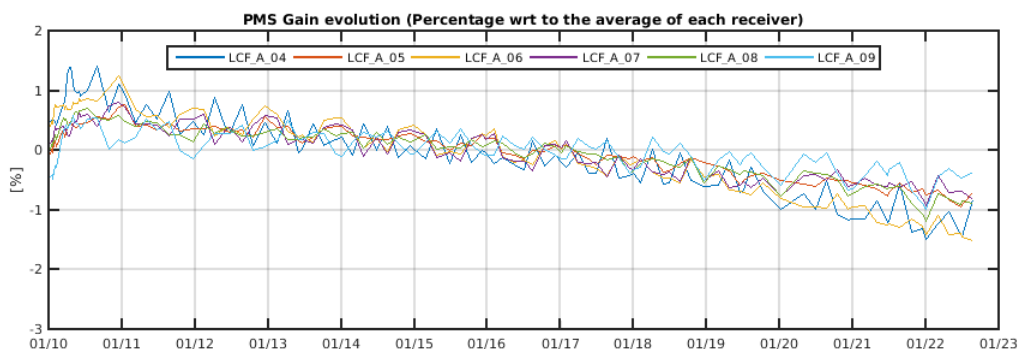


Figure 10 Evolution of the Δ PMS Gain of the LICEFS in CMN A1

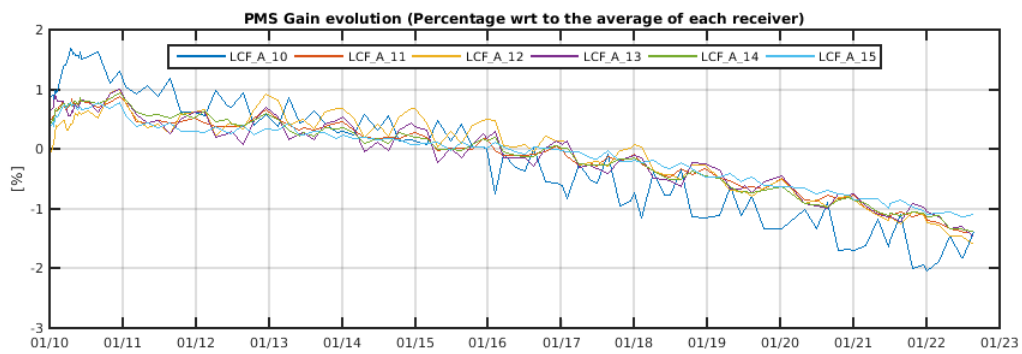


Figure 11 Evolution of the Δ PMS Gain of the LICEFS in CMN A2

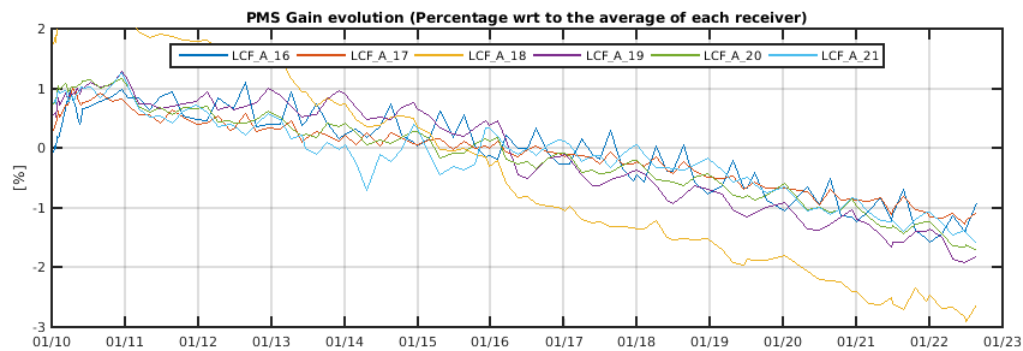


Figure 12 Evolution of the Δ PMS Gain of the LICEFS in CMN A3

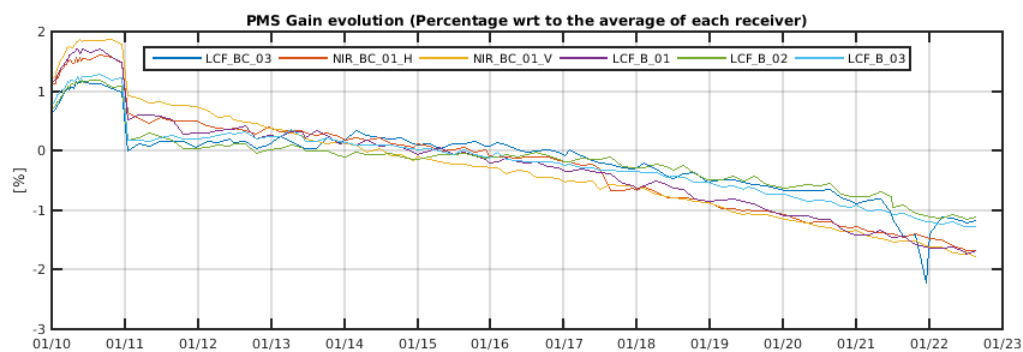


Figure 13 Evolution of the Δ PMS Gain of the LICEFS in CMN H2

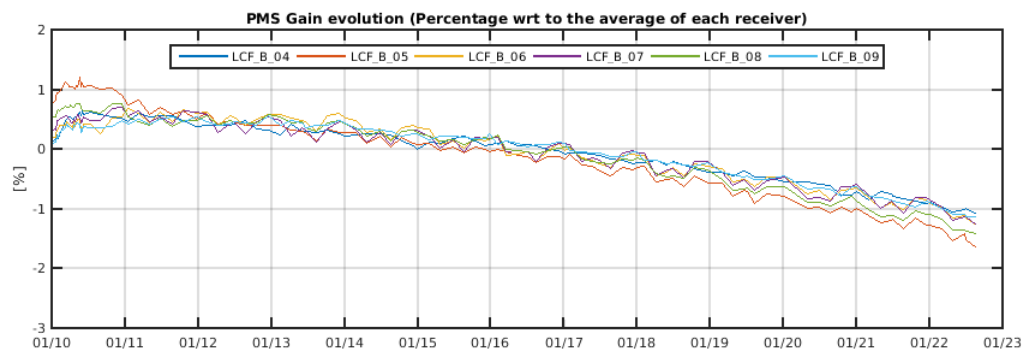


Figure 14 Evolution of the Δ PMS Gain of the LICEFS in CMN B1

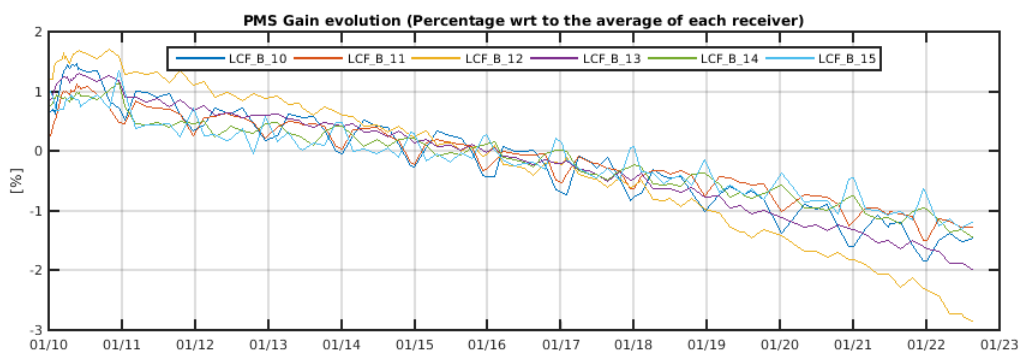


Figure 15 Evolution of the Δ PMS Gain of the LICEFS in CMN B2

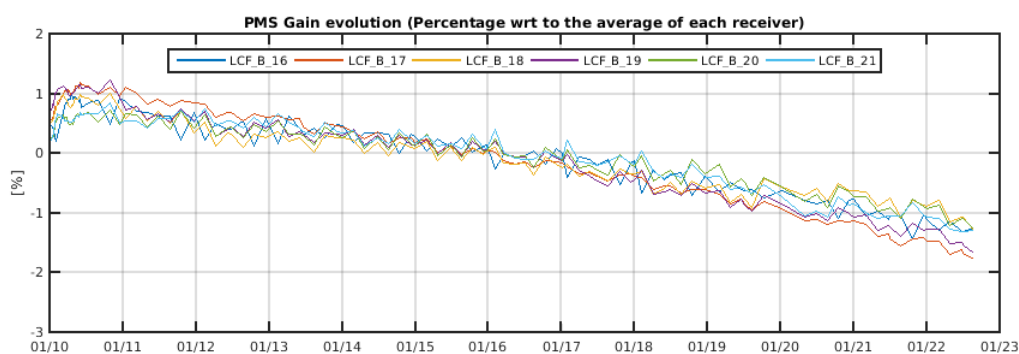


Figure 16 Evolution of the Δ PMS Gain of the LICEFS in CMN B3

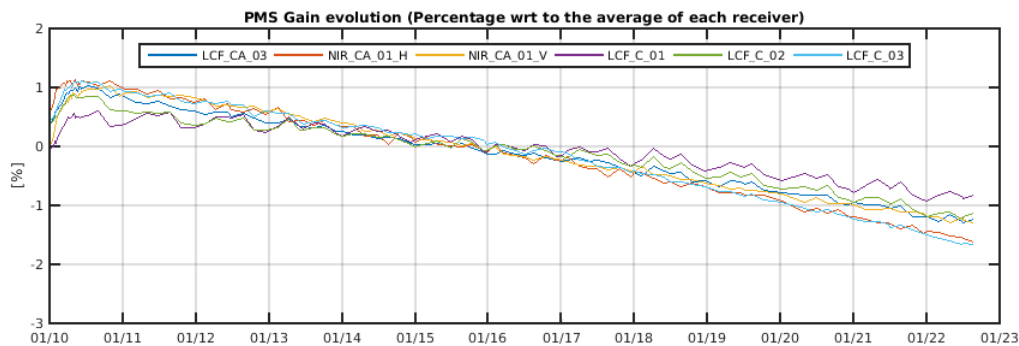


Figure 17 Evolution of the Δ PMS Gain of the LICEFS in CMN H3

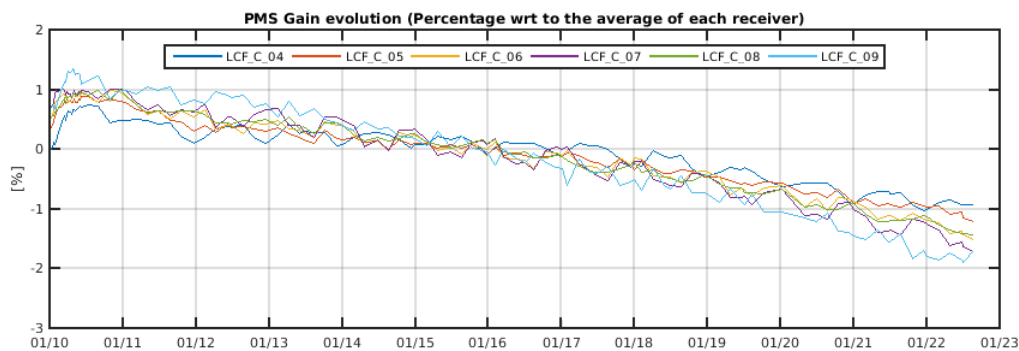


Figure 18 Evolution of the Δ PMS Gain of the LICEFS in CMN C1

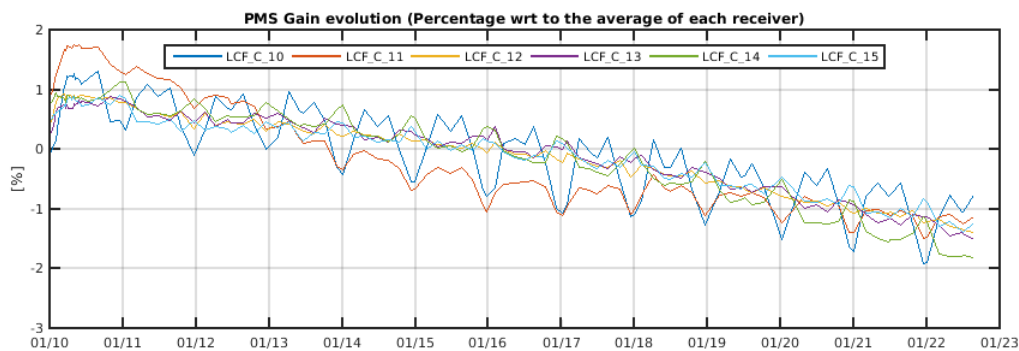


Figure 19 Evolution of the Δ PMS Gain of the LICEFS in CMN C2

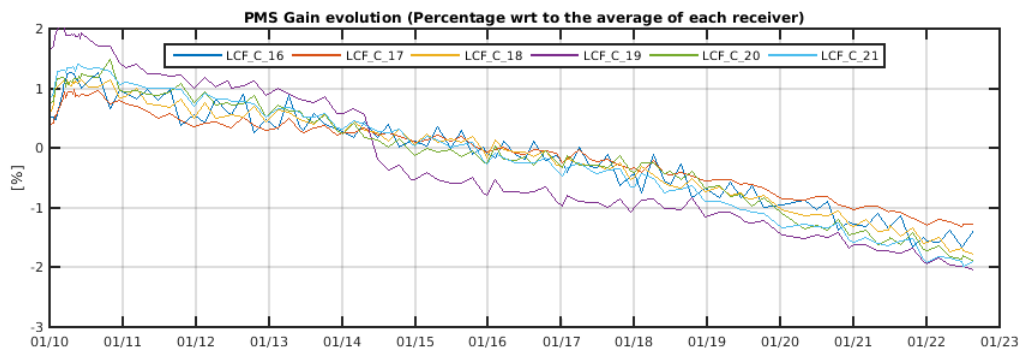


Figure 20 Evolution of the Δ PMS Gain of the LICEFS in CMN C3

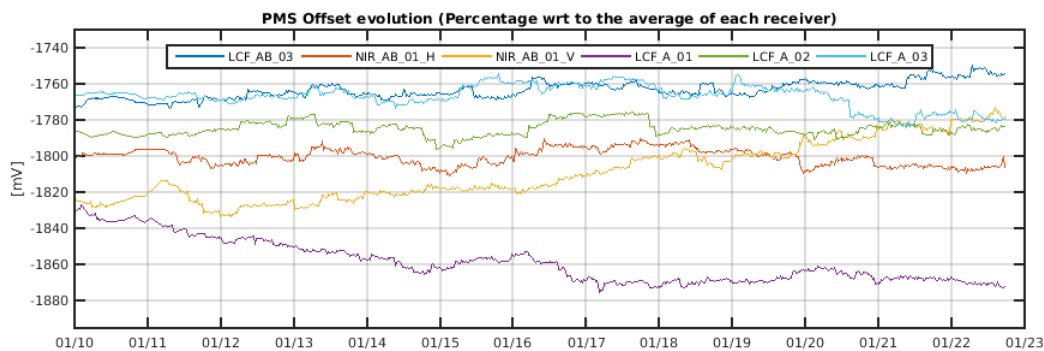


Figure 21 Evolution of the Δ PMS Offset of the LICEFS in CMN H1

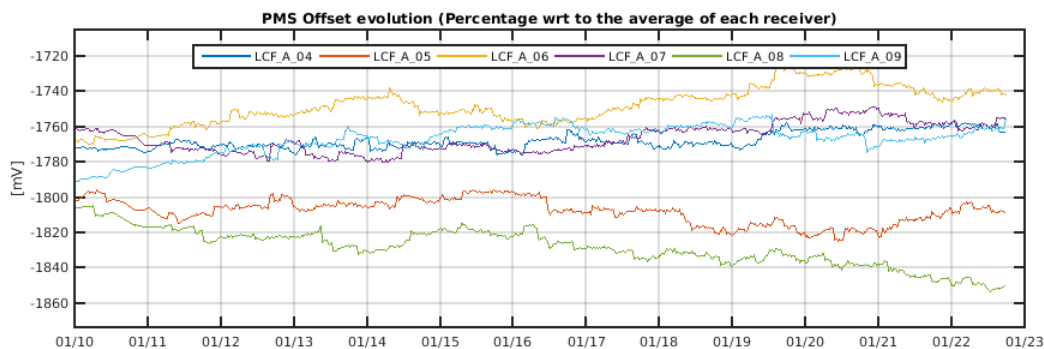


Figure 22 Evolution of the Δ PMS Offset of the LICEFS in CMN A1

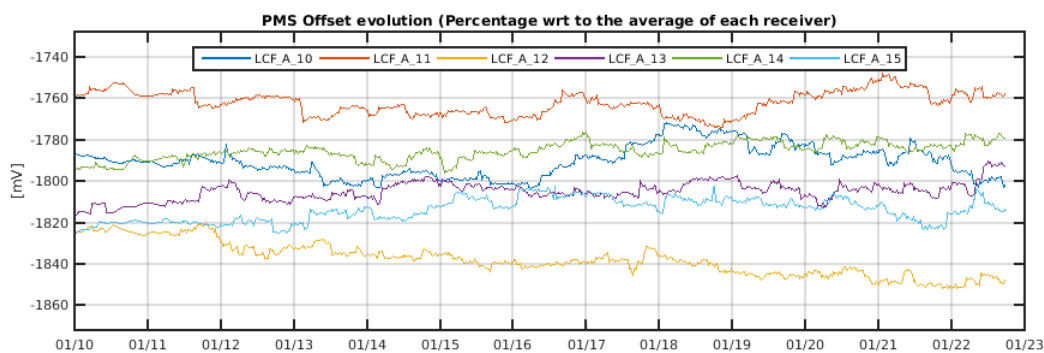


Figure 23 Evolution of the Δ PMS Offset of the LICEFS in CMN A2

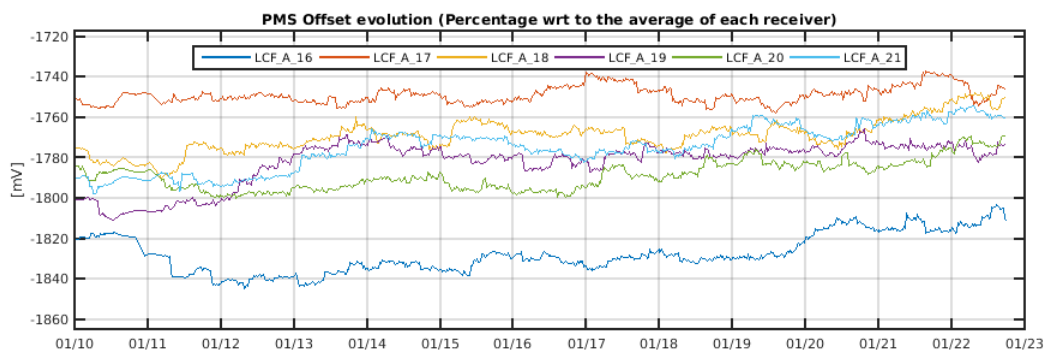


Figure 24 Evolution of the Δ PMS Offset of the LICEFS in CMN A3

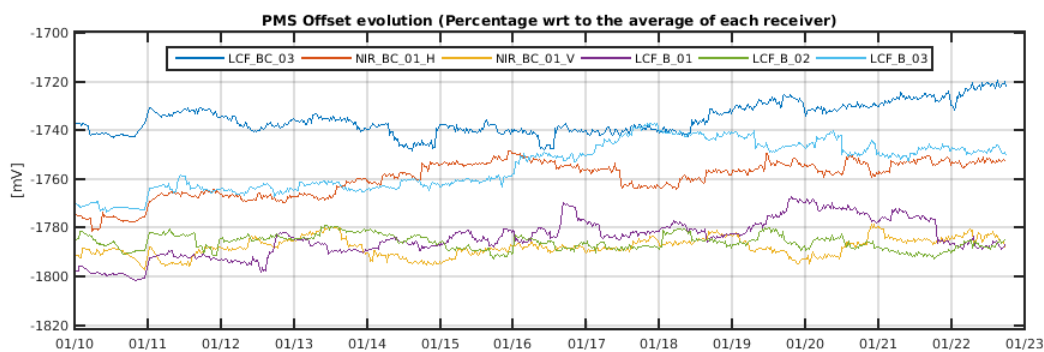


Figure 25 Evolution of the Δ PMS Offset of the LICEFS in CMN H2

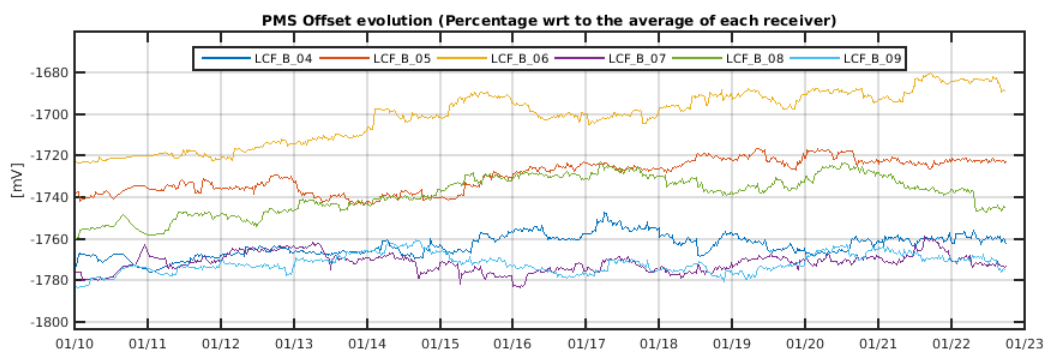


Figure 26 Evolution of the Δ PMS Offset of the LICEFS in CMN B1

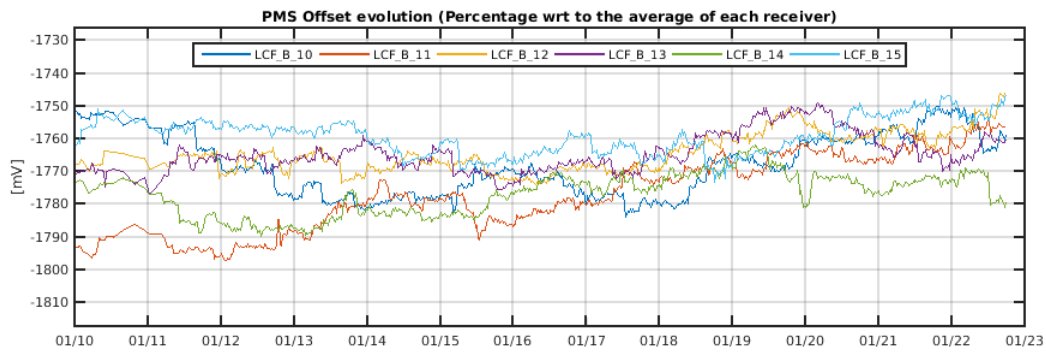


Figure 27 Evolution of the Δ PMS Offset of the LICEFS in CMN B2

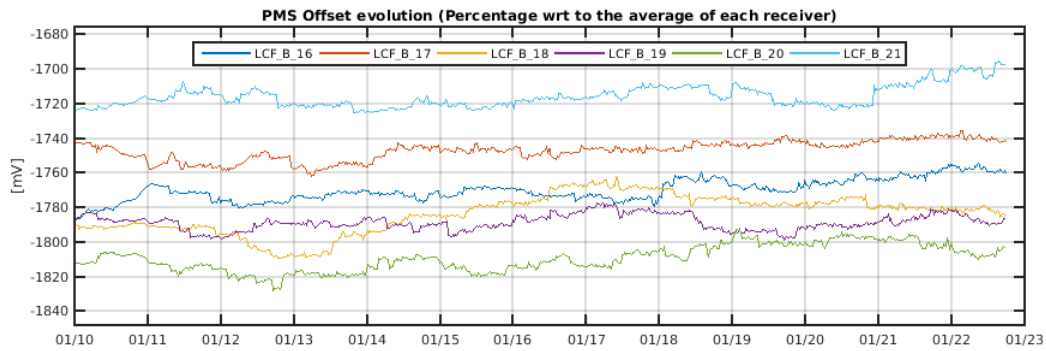


Figure 28 Evolution of the Δ PMS Offset of the LICEFS in CMN B3

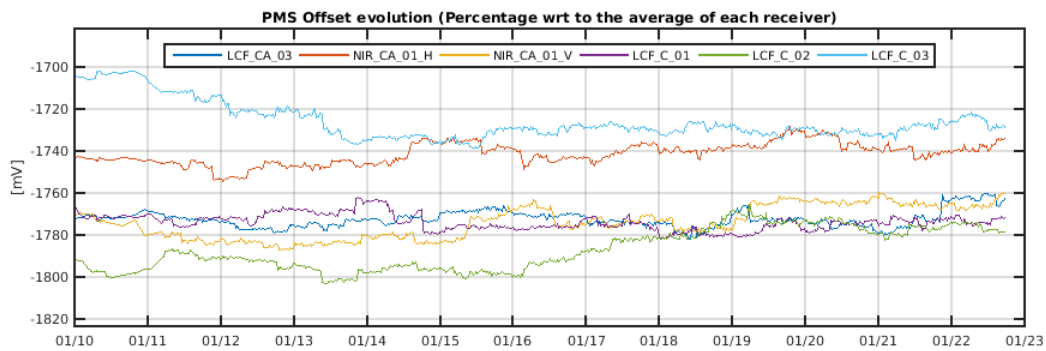


Figure 29 Evolution of the Δ PMS Offset of the LICEFS in CMN H3

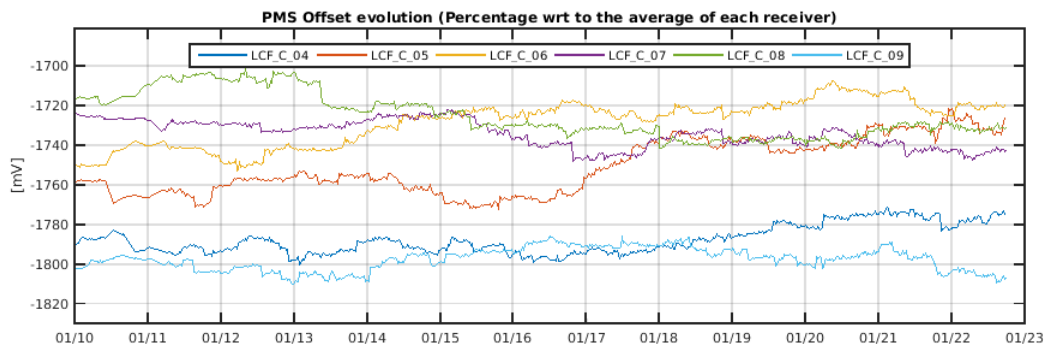


Figure 30 Evolution of the Δ PMS Offset of the LICEFS in CMN C1

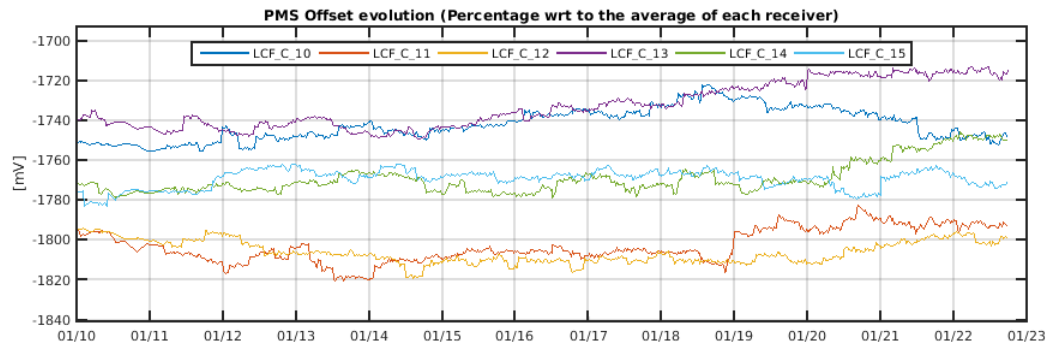


Figure 31 Evolution of the Δ PMS Offset of the LICEFS in CMN C2

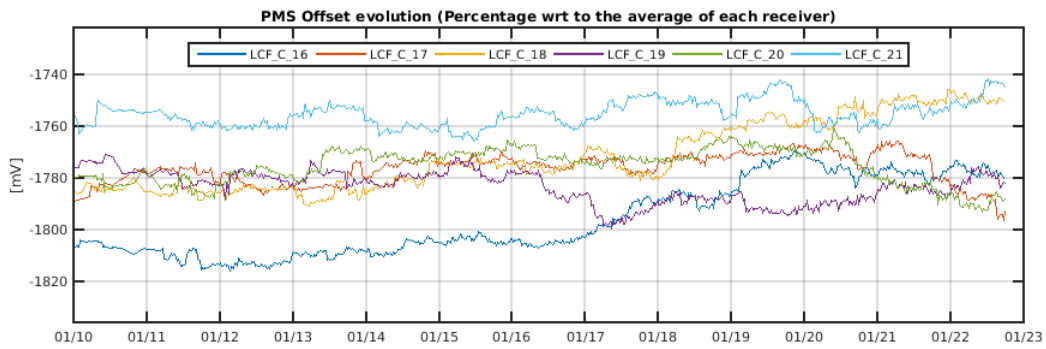


Figure 32 Evolution of the Δ PMS Offset of the LICEFS in CMN C3

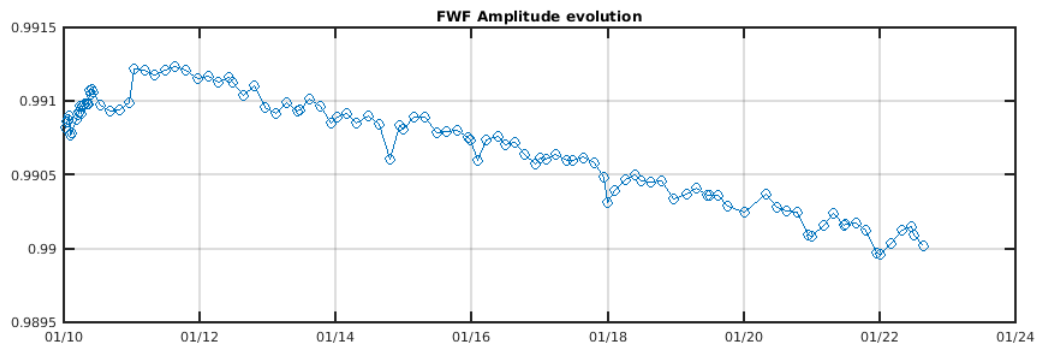


Figure 33 Evolution of the average of the FWF Amplitude at the origin

The evolution of the average of the correlator offsets does not show any significant drift. Also, the correlation offsets between receivers that do not share local oscillator remains much smaller than the correlation offsets between receivers sharing local oscillator. This result is expected since any residual correlated signal arriving to a pair of receivers, arrives through the local oscillator signal.

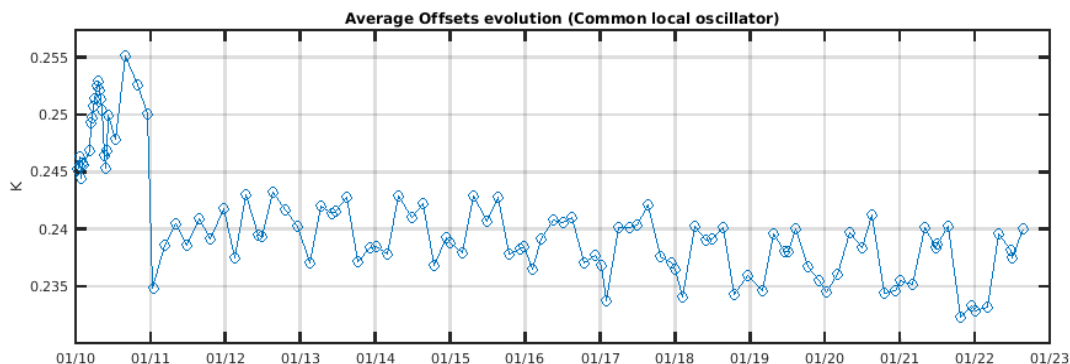


Figure 34 Evolution of the average of the Correlator offsets for the baselines which share local oscillator

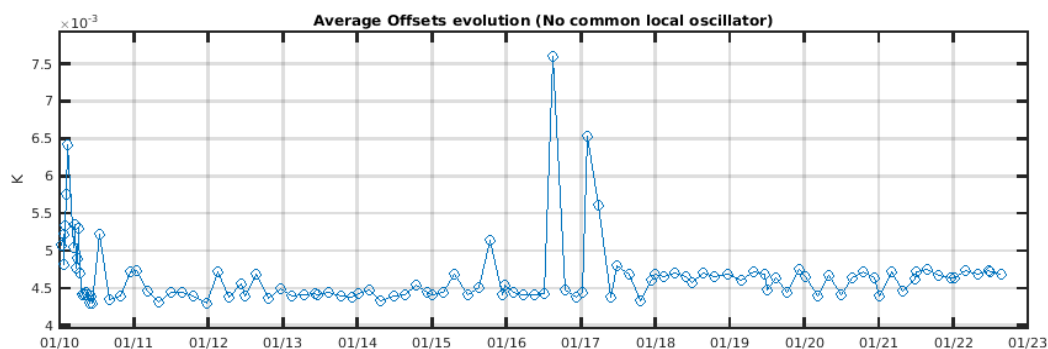


Figure 35 Evolution of the average of the Correlator offsets for the baselines which do not share local oscillator

5.3 Brightness Temperatures Trends over Dome-C Point (Antarctic)

The result of the monitoring of the evolution of the SMOS brightness temperature over Dome-C is shown in the Figure 36 (X and Y polarization at antenna frame for all the incidence angles) and in Figure 37, Figure 38 (H and V polarization at surface level for 42.0 degrees incidence angle for different areas of the Field of View). The values are averaged every 18 days to reduce the noise and the value for July 2010 is subtracted and used as relative reference. In figure 37 are also shown in situ measurements (Dome-C) from the DOMEX experiment averaged on the same period of the SMOS data. DOMEX data for year 2017 has been calibrated with a more accurate and refined procedure, this explains the bias with reference to previous year acquisition. The residual long-term drift in 2017 is due to drift in calibration parameters. Therefore, is not a geophysical effect and it will be corrected in the next delivery of DOMEX data.

The evolution of the SMOS brightness temperature trend over Dome-C does not show any significant drift except for two events, in H polarization, at the beginning of 2015 and in March 2020. The increase in Brightness temperature in 2015 was due to a change on surface geophysical condition: accumulation of snow since November 2014 and rapidly evolution of snow density on 22 March 2015 when a strong wind had changed the surface condition. This event has impacted the emissivity of the ice that was confirmed by on-site L-band measurement (DOMEX experiment) and from the Aquarius data set. The decrease in Brightness Temperature in March 2020 is confirmed to be related to

changes in surface geophysical condition, since analysis of SMAP data over the same area shows similar trend in H polarisation. Further details can be found at 'Influence of snow surface properties on L-band brightness temperature at Dome C' paper published by IFAC-CNR, Grenoble Alpes University and CESBIO (<https://doi.org/10.1016/j.rse.2017.07.035>).

The SMOS brightness temperature V polarization measurements are quite stable since the beginning of the mission. The SMOS brightness temperature H polarization measurements are less stable and impacted by geophysical condition at surface level. Thus, the drop of the latter for the reporting month is under investigation.

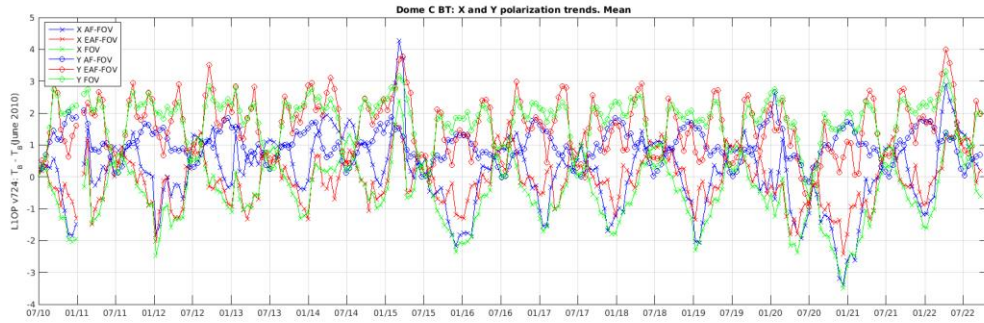


Figure 36: Dome-C X and Y polarization trends (all incidence angles).

FOV: statistics computed for Dome-C grid point located in any position of the retrieved image (excluding alias images borders). AF: statistics computed for Dome-C grid point located only in the position of the retrieved image not impacted by alias (alias free area). EAF-FOV: statistics computed for Dome-C grid point located only in the position of the retrieved image where the alias free area has been extended.

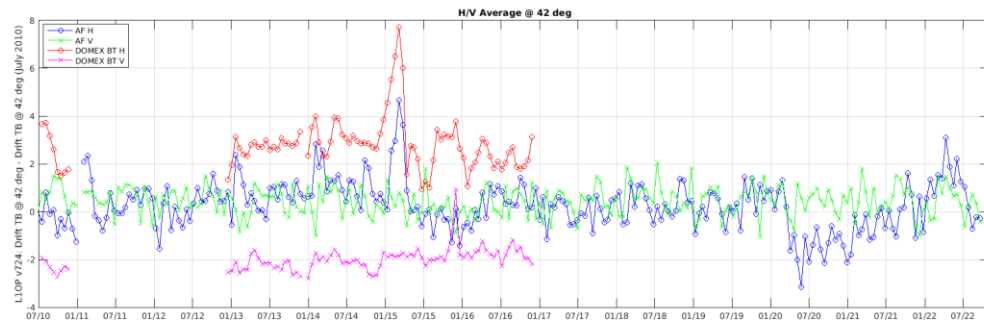


Figure 37: Dome-C H and V polarization trends in Alias Free zone (incidence angle 42°)

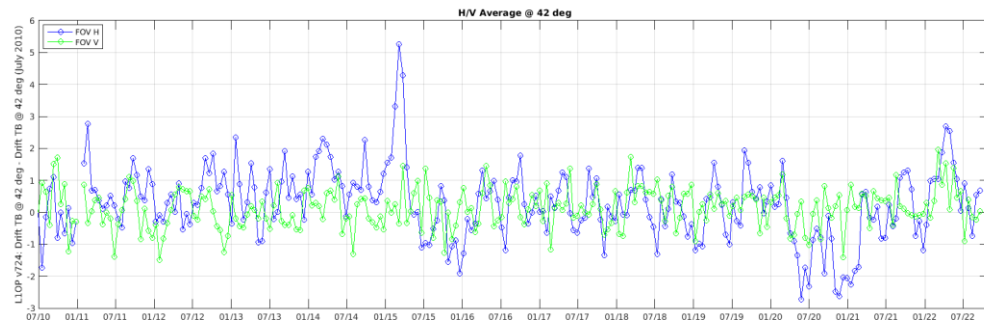


Figure 38: Dome-C H and V polarization trends in Extended Alias Free zone (incidence angle 42°)

5.4 Brightness Temperature Stability over the ocean:

SMOS Brightness Temperature Stability over the ocean is monitored by comparison of SMOS measurements with the forward ocean model. The initial monitoring based on Sea Surface Salinity derived by monthly fixed map from World Ocean Atlas model (WOA2009) has been upgraded with the usage of In-Situ Analysis System (ISAS) measurements interpolated by Objective Analysis (OA). With the new approach, geophysical effects in the difference between SMOS measurements and ocean model has been greatly mitigated allowing a better instrument calibration monitoring. Due to the complexity of the monitoring and the off-line availability of ISAS-OA dataset, the results are available till March 2020. Results will be updated on a yearly basis.

The result of the monitoring of the evolution of the SMOS brightness temperature over the ocean is shown in the Figures 40-43 as a Hövmoller plot (time-latitude plot with averaged longitudes for the Brightness Temperature anomaly with respect to the ocean model).

The latitude-longitude area is defined as described in figure 39. This aims to obtain a sufficiently large water body without much interfering land masses, land sea contamination, RFI presence, etc, to be used as a well-known reference. For that area, the ocean model is deemed sufficiently known.

In addition to the Hövmoller plots, several additional metrics are provided. Figures 44-47 contain trends computed over the Hövmoller for several areas of interest. They contain latitude-longitude Brightness Temperature averages evolution.

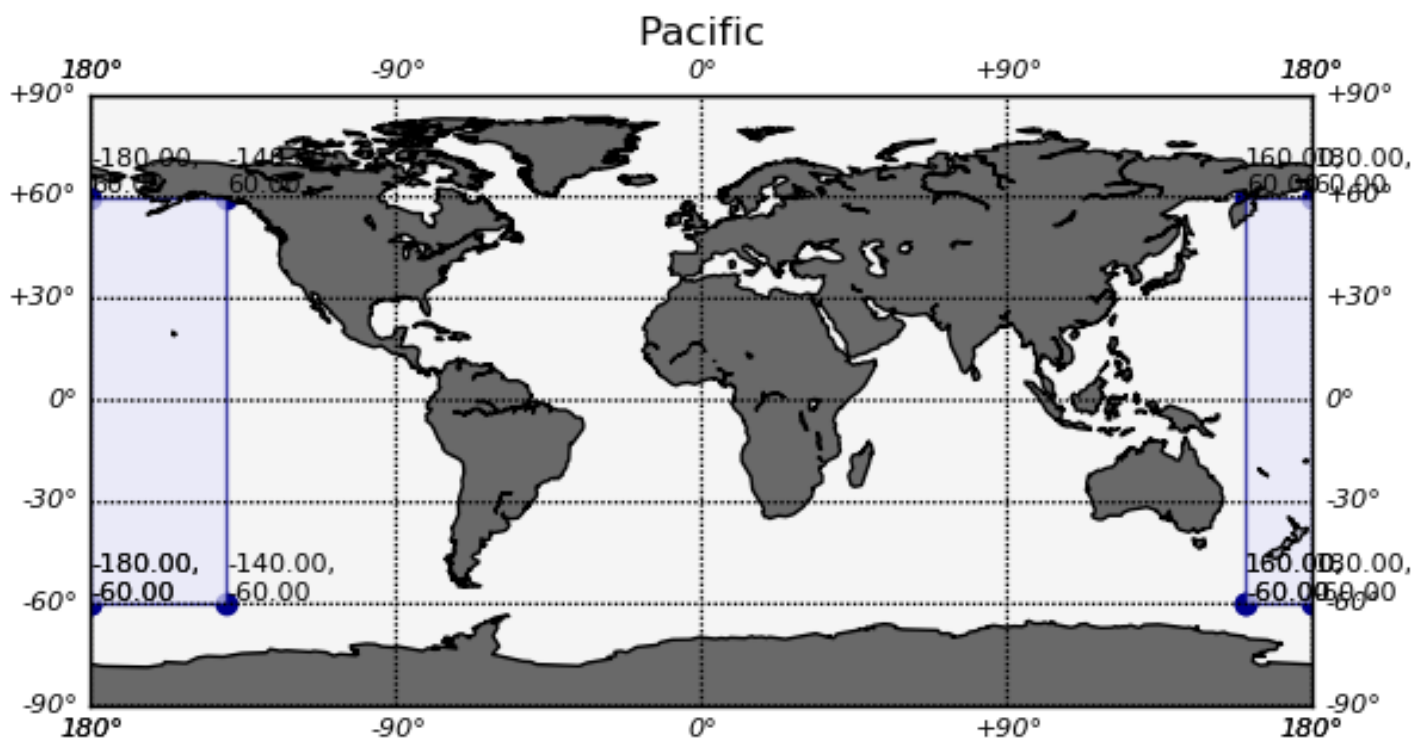


Figure 39: Open Ocean region used for the Hövmoller computation.

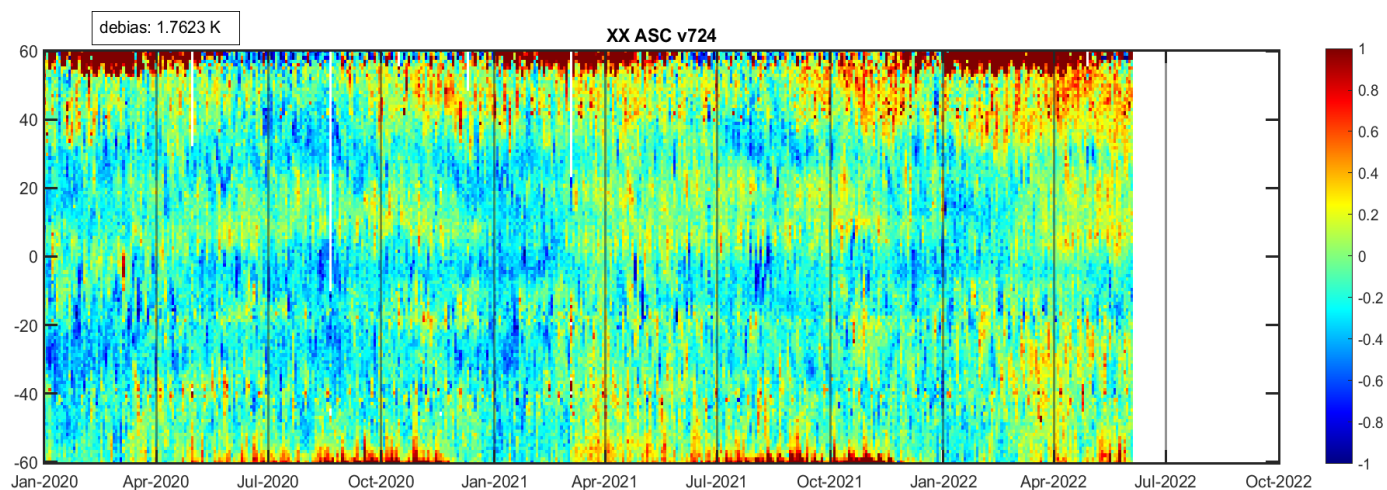


Figure 40: BT stability over the ocean, for XX polarization and Ascending passes in Kelvin.

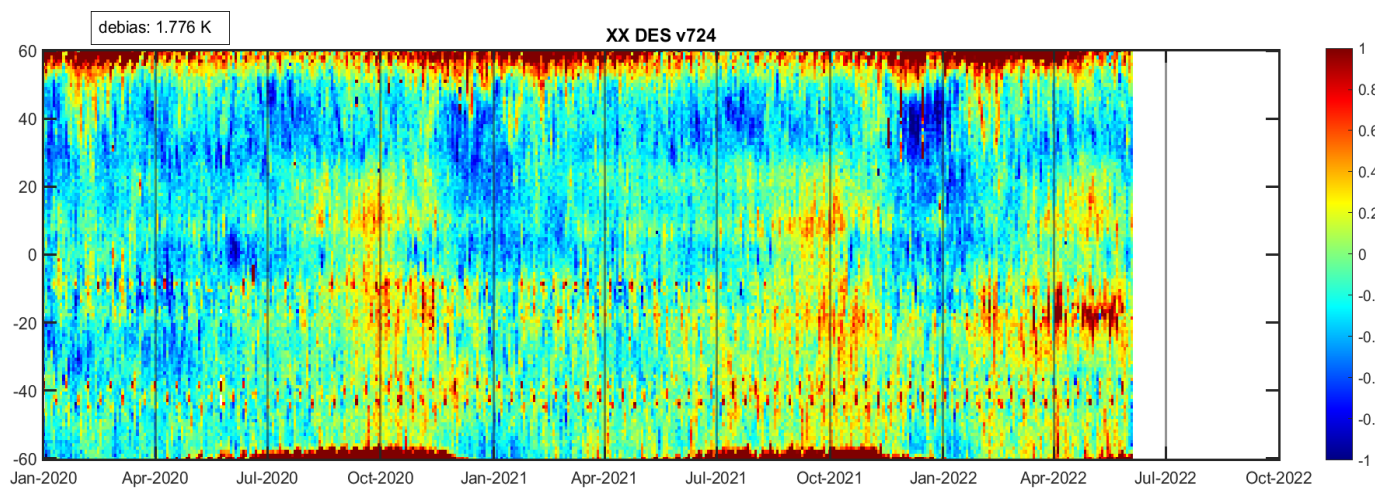


Figure 41: BT stability over the ocean, for XX polarization and Descending passes in Kelvin.

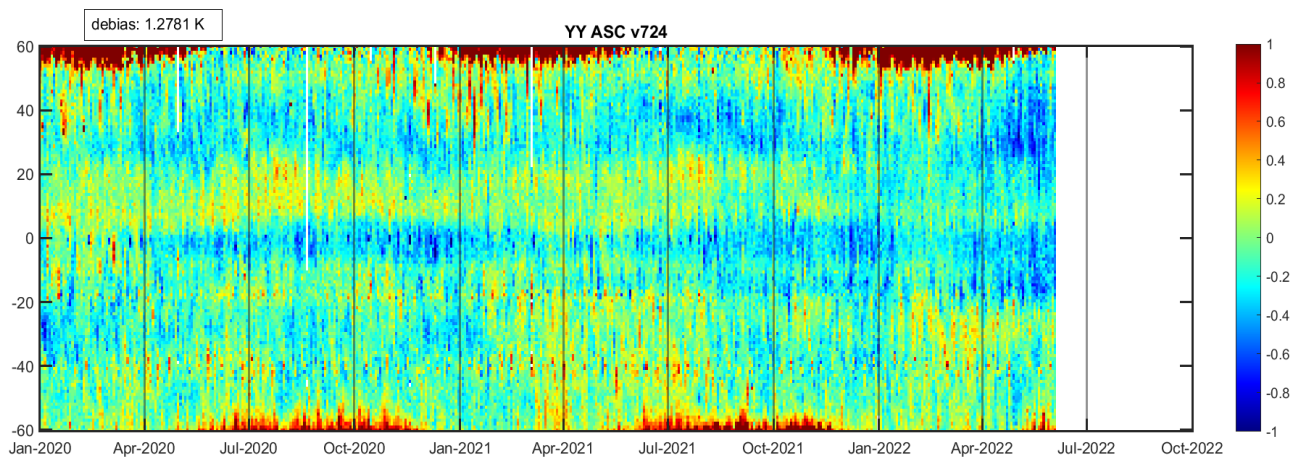


Figure 42: BT stability over the ocean, for YY polarization and Ascending passes in Kelvin.

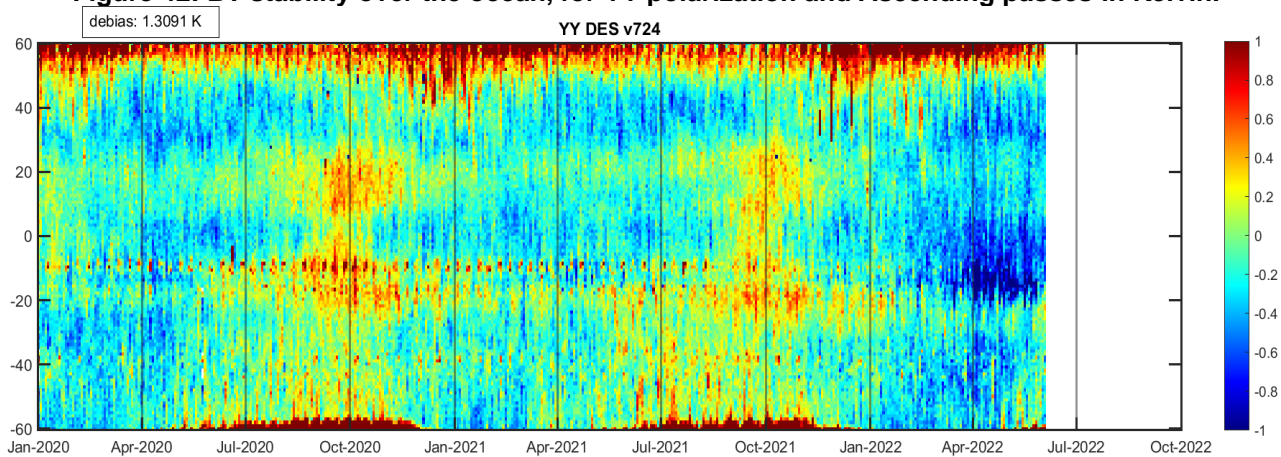


Figure 43: BT stability over the ocean, for YY polarization and Descending passes in Kelvin.

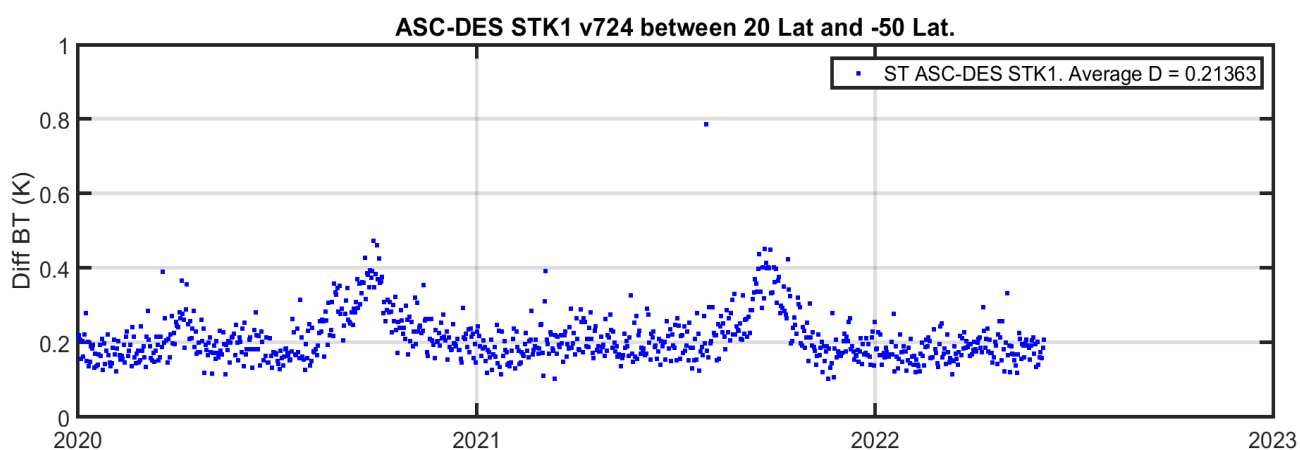


Figure 44: BT short-term stability trends (ASC-DES) for Stokes 1, XX and YY polarizations

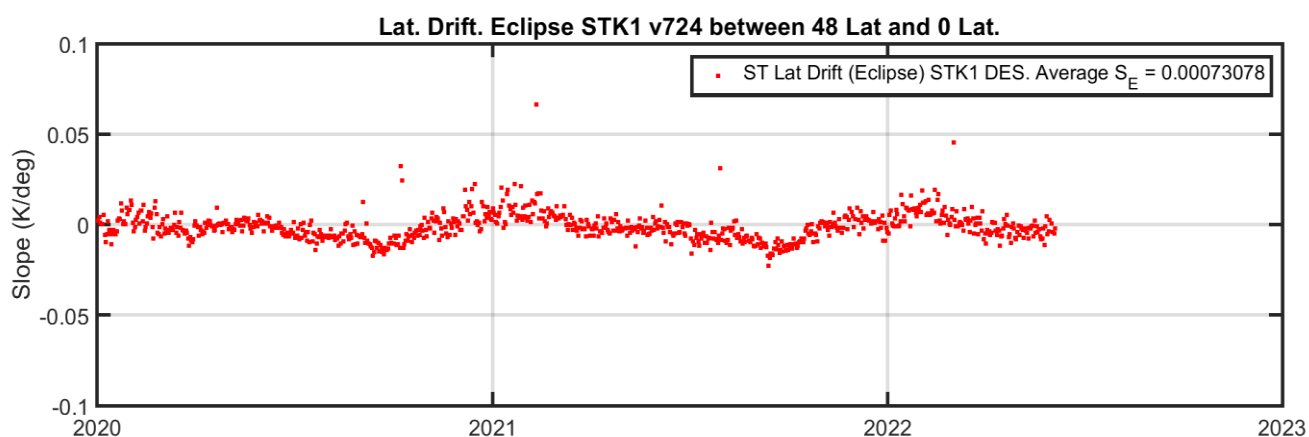


Figure 45: BT short term stability at Eclipse regions, for Stokes 1, XX and YY polarizations

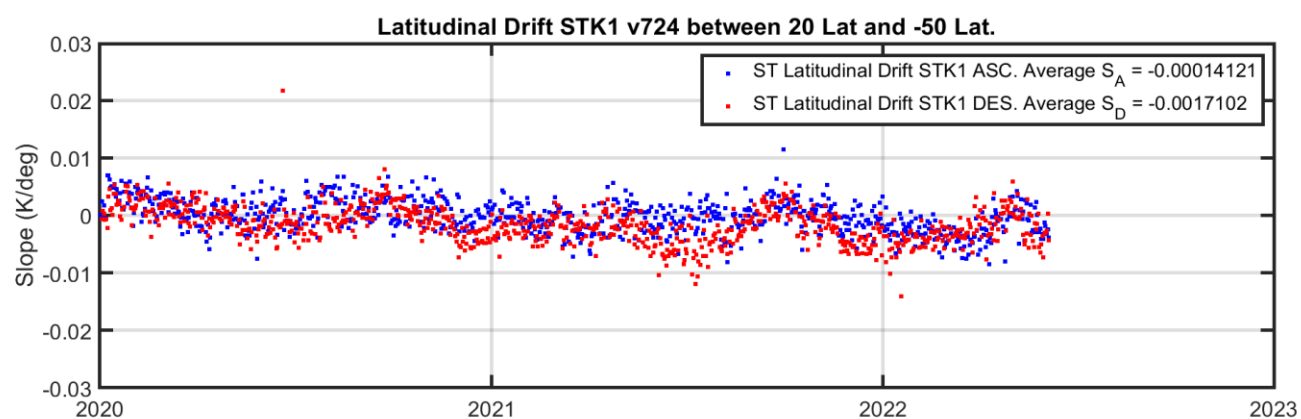


Figure 46: BT short term stability (Latitudinal drift) for ASC-DES Stokes 1, XX and YY polarizations.

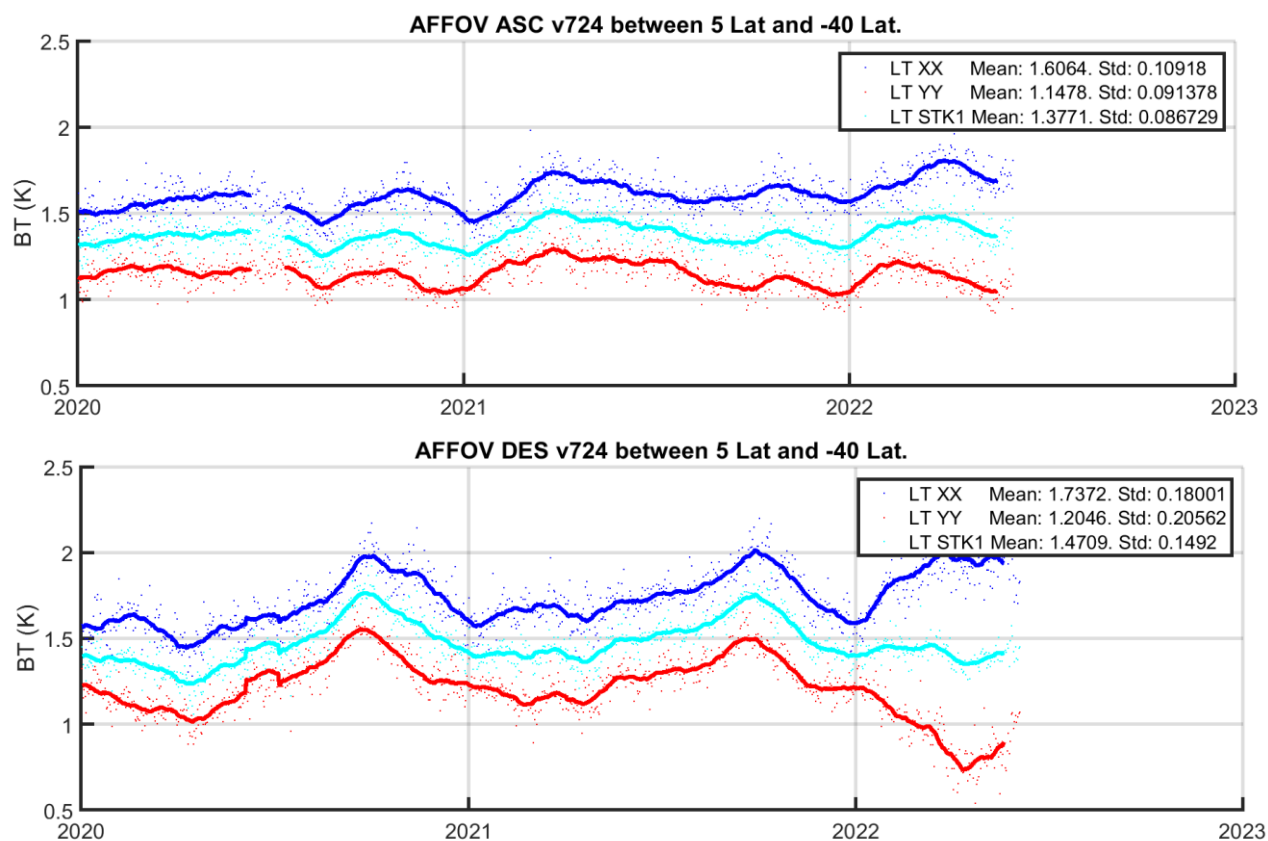


Figure 47: BT long term stability (ASC/DES), for XX and YY polarizations, and Stokes 1.

5.5 L1C Quality Parameter Analysis

This section provides a long-term overview of the monitoring of the L1C quality parameters, to identify major problems and trends.

The L1C quality flags have been extracted for the whole dataset. The L1C quality flags identify the total number of degraded measurements (snapshots) which have been affected by software, instrument, auxiliary data (ADF) or calibration errors. They provide a way to assess the degradation of a particular measurement and product and to help to identify its causes.

A daily average of the number of degraded measurements per MIR_SCxx1C file (product) has been selected as a metric. This provides an estimation of the mean number of degraded snapshots per file (product) for each day:

$$\text{Mean number of degraded snapshot per product} = \frac{\text{total number of degraded snapshots per day}}{\text{total number of products per day}}$$

The metric is also given in relative percentage with respect the total number of snapshots in that day:

$$\text{Percentage of degraded snapshots per day} = 100 \times \frac{\text{total number of degraded snapshots per day}}{\text{total number of snapshots that day}}$$

The metric is computed for ascending and descending orbit direction separately. In case the percentage of degraded snapshots per day is not negligible (e.g., above 2%) a detailed analysis of the dataset is performed to identify the root cause of the degradation for that day.

5.5.1 Software Errors

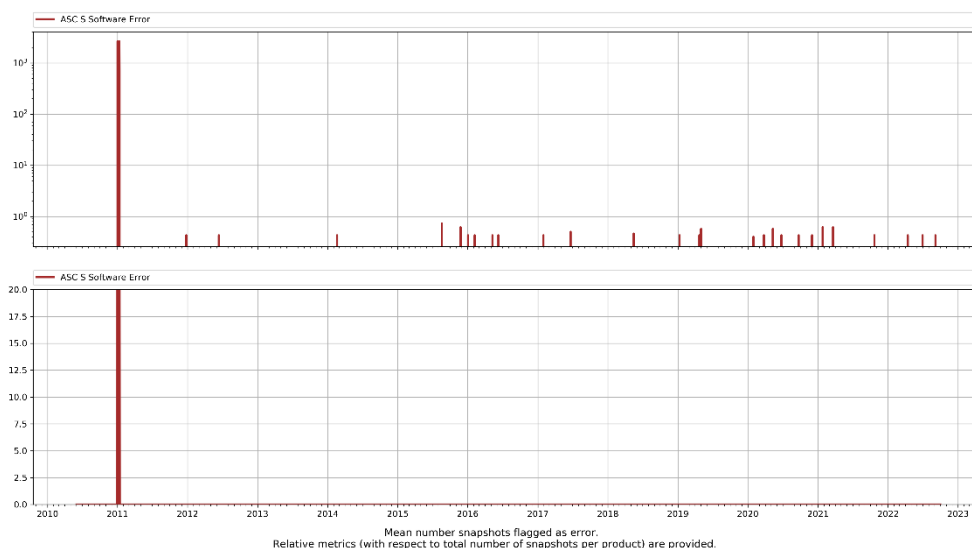


Figure 48: L1C V724 Software Errors Ascending Orbits

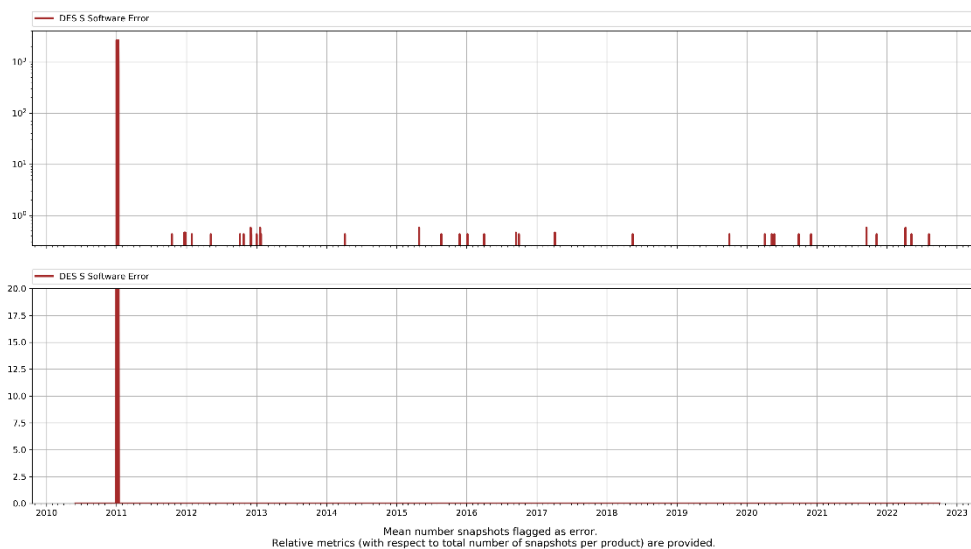


Figure 49: L1C V724 Software Errors Descending Orbits

This error summarizes several exceptions that the SW may encounter, such as interpolation problems, denominator equal to 0, out-of-bound parameters, etc (see [RD1](#) for more comprehensive detailed description). Only few software errors were logged for the entire dataset. The exception is Jan 2011, which were originated on the instrument anomaly, and May 2010, during commissioning phase (origin under investigation). After Jan 2011, the number of affected snapshots is negligible.

5.5.2 Instrument Errors

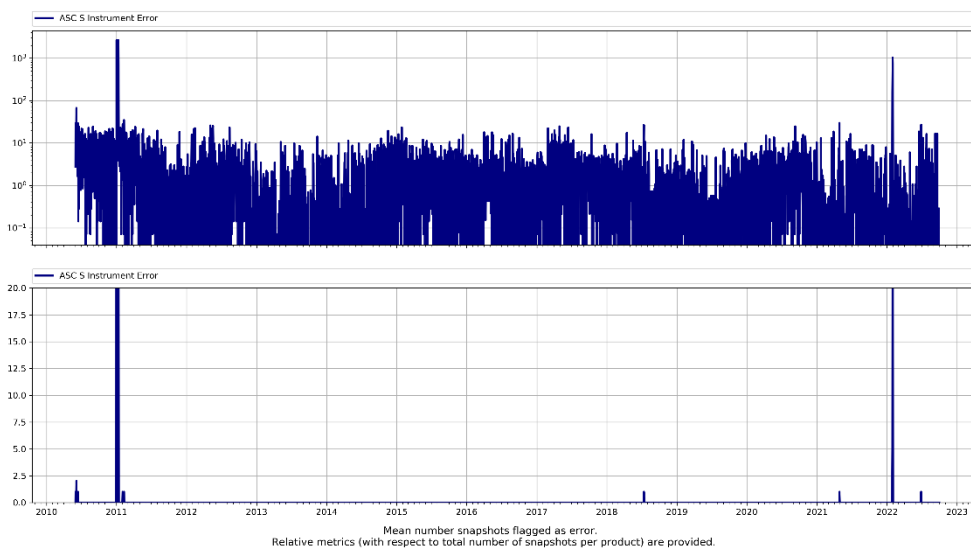


Figure 50: L1C V724 Instrument Errors Ascending Orbits

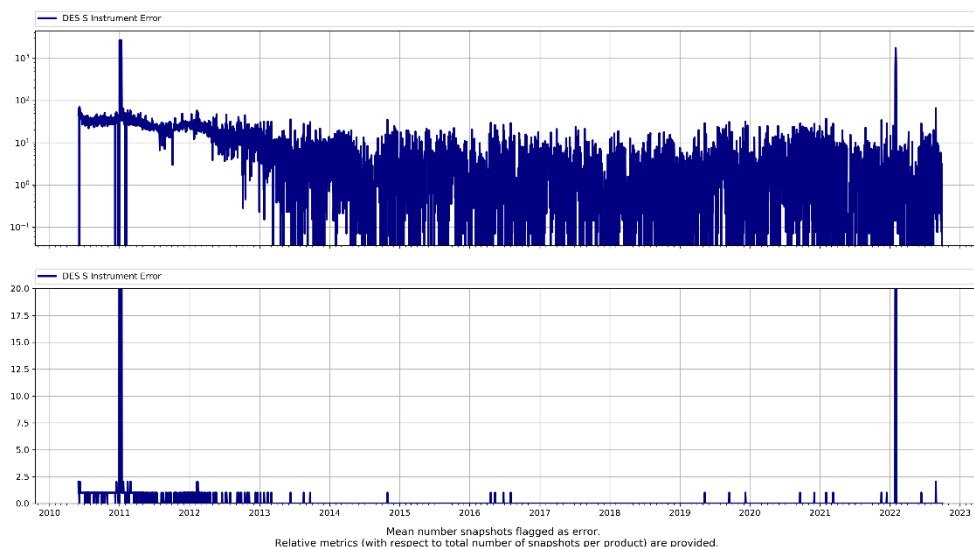


Figure 51: L1C V724 Instrument Errors Descending Orbits

This error signals instrument anomalies that could have impact in data quality (see [RD1](#) for more comprehensive detailed description). In addition, it has been discovered that severe RFI may trigger this error flag as well: In some cases, RFIs sources strongly degrades the instrument correlation measurement. This degradation impacts the number of iterations required to converge in the internal L1A correlation correction and therefore is flagged as potential instrument error and further propagated to L1C product. Also, it should be mentioned that instrument errors might also be triggered by the increase of Arm-A temperatures during eclipse seasons, this is the case for the peak during January 2022: LICEF-A4 slightly surpassed the threshold of 29°C used to set the flag.

Besides commissioning period (May 2010), the instrument anomaly in January 2011 and the increase of Arm-A temperatures by the end of January 2022 and beginning of February 2022 (eclipse season), the number of flagged snapshots is very low, always being < 2.5%. An interesting drift is observed for the Instrument Error flag for Descending passes, as it clearly shows a progressive reduction of the number of corrupted snapshots from an average of 50 affected snapshots per day to an average of five. This can be related with the removal of on ground RFIs sources with respect the beginning of the mission. Interesting enough, the same trend cannot be appreciated for Ascending passes. This can be associated with the fact that reduction of RFI was particularly intense for some North American sources that mainly affected descending passes.

5.5.3 ADF Errors

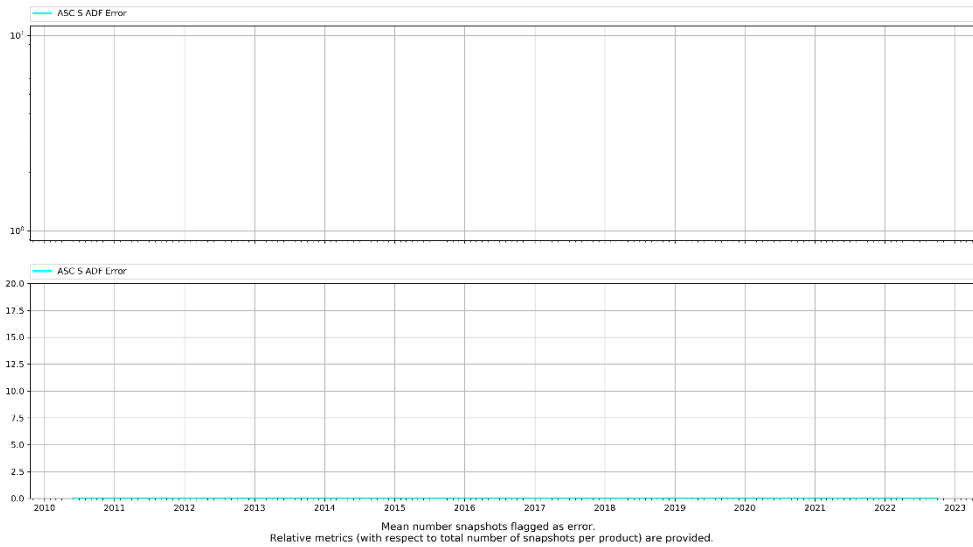


Figure 52: L1C V724 ADF Errors Ascending Orbits

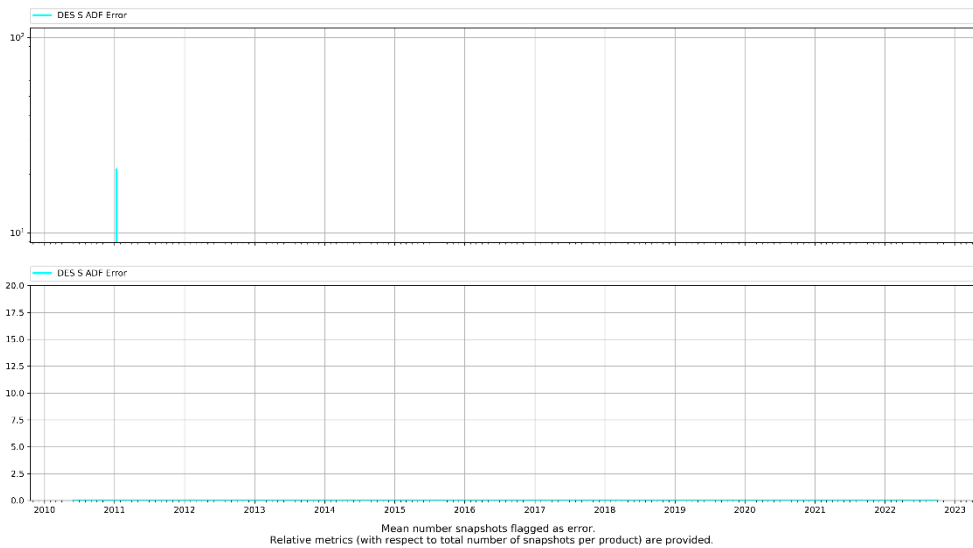


Figure 53: L1C V724 ADF Errors Descending Orbits

ADF Errors count the number of snapshots affected by Auxiliary Data anomalies (see [RD1](#) for more comprehensive detailed description). No significant number of ADF errors are logged for the entire dataset. The exception is Jan 2011, which were originated on the instrument anomaly. Some other products from 2010 to 2015 present ADF errors coming from no AUX_RFILST data available. This issue only affects some snapshots one product each change of month (see plot below), and it is caused by a non-enough overlapping of the input 2010-2015 AUX_RFILST dataset.

5.5.4 Calibration Errors

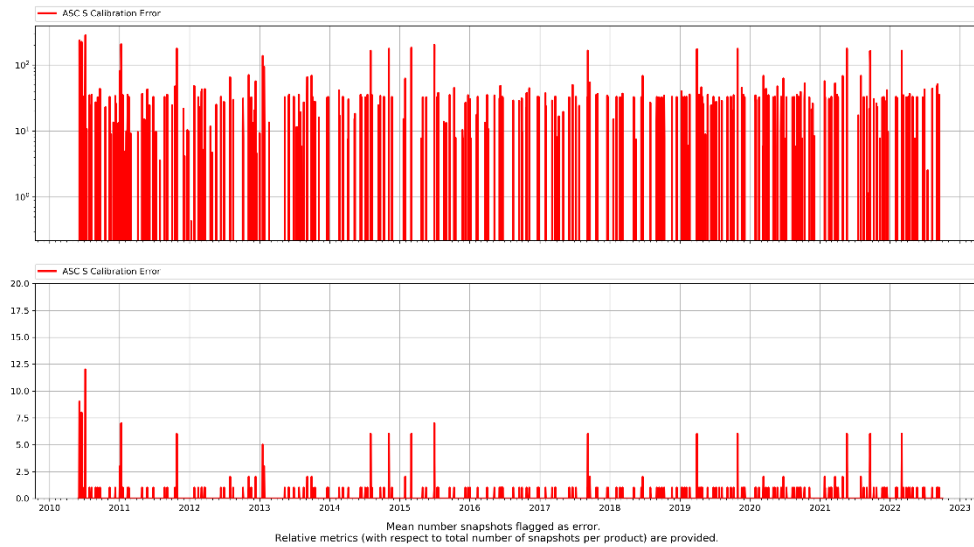


Figure 54: L1C V724 Calibration Errors Ascending Orbits

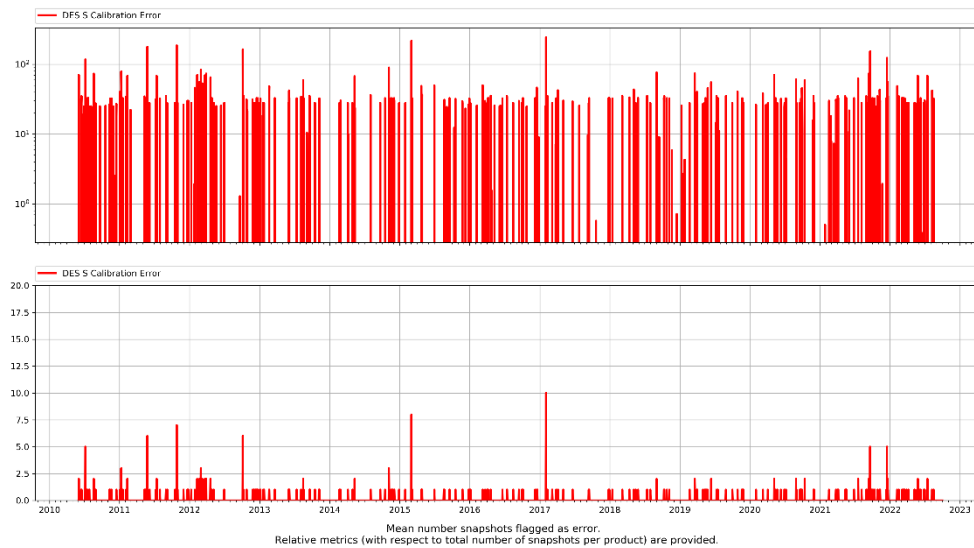


Figure 55: L1C V724 Calibration Errors Descending Orbits

Calibration errors summarize diverse errors related to calibration sequences usage (see [RD1](#) for more comprehensive detailed description). Calibration errors are consistent across the mission, generally affecting less than to the 1% of the sequences every day. In selected dates, however, anomalies that are more serious can be appreciated, affecting up to 5% of the snapshots.

For the rest of the dataset, calibration errors are commonly triggered due to events causing gaps in the Local Oscillator calibrations (CSTD1A) or degraded calibration data due to CMN Unlocks. Specific detail for each product affected by calibration errors can be found in RD1 inside 'ALL FULL Degraded Products' section. Additionally, it should be mentioned that most of the products proposed inside the 'Main FULL Degraded Products' section to be discarded are the ones affected by calibrations errors.

5.5.5 Invalid Blocks

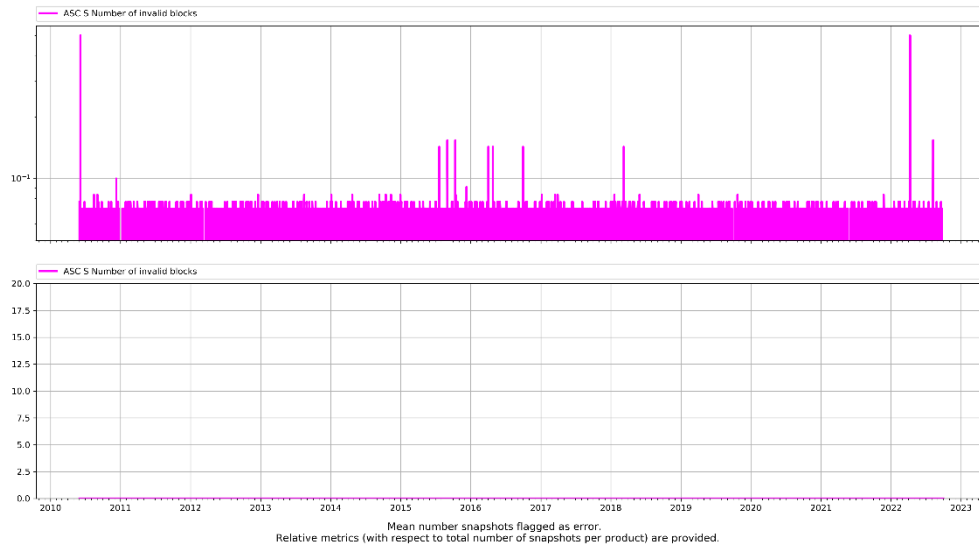


Figure 56: L1C V724 Invalid Blocks Ascending Orbits

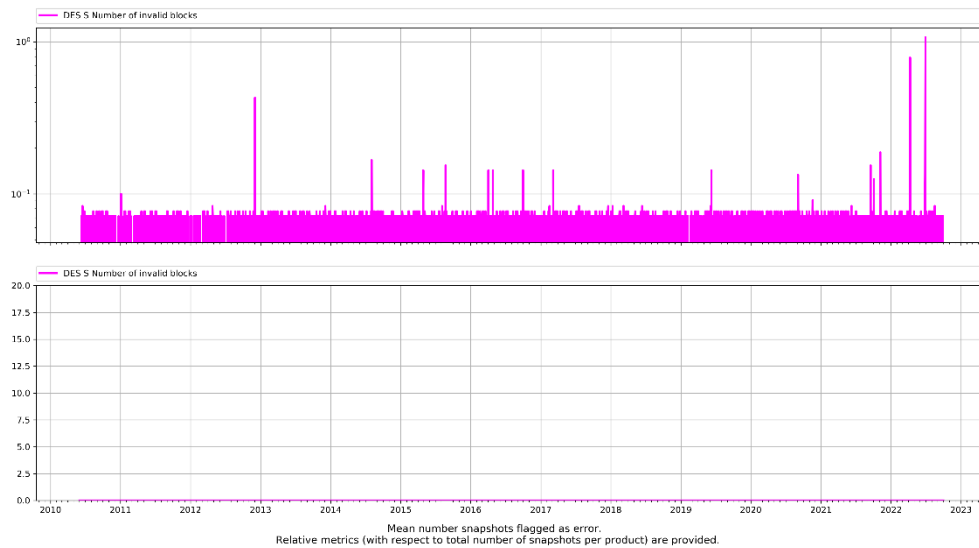


Figure 57: L1C V724 Invalid Blocks Descending Orbits

The invalid blocks flag counts the number of blocks of 24 packets in the corresponding L0 product that have at least one invalid packet (see [RD1](#) for more comprehensive detailed description). Albeit some packets are regularly flagged as invalid, the number of flagged packets is negligible for the entire dataset. The peak in June 2022 is related to incomplete pass acquire in Svalbard, data was recovered within the next pass. It is expected the peak disappears once the recovered data have been regenerated.

5.5.6 Discarded Scenes

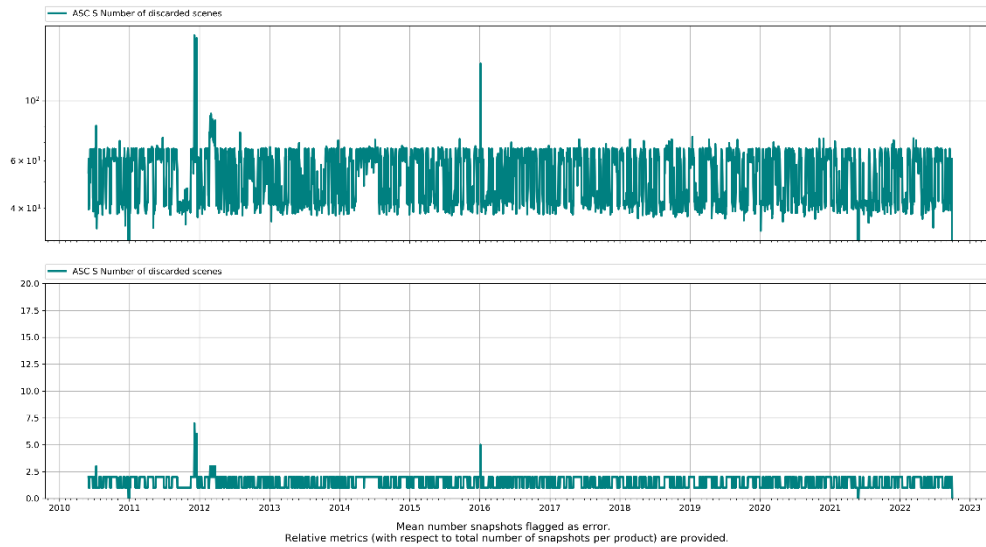


Figure 58: L1C V724 Discarded Scenes Ascending Orbits

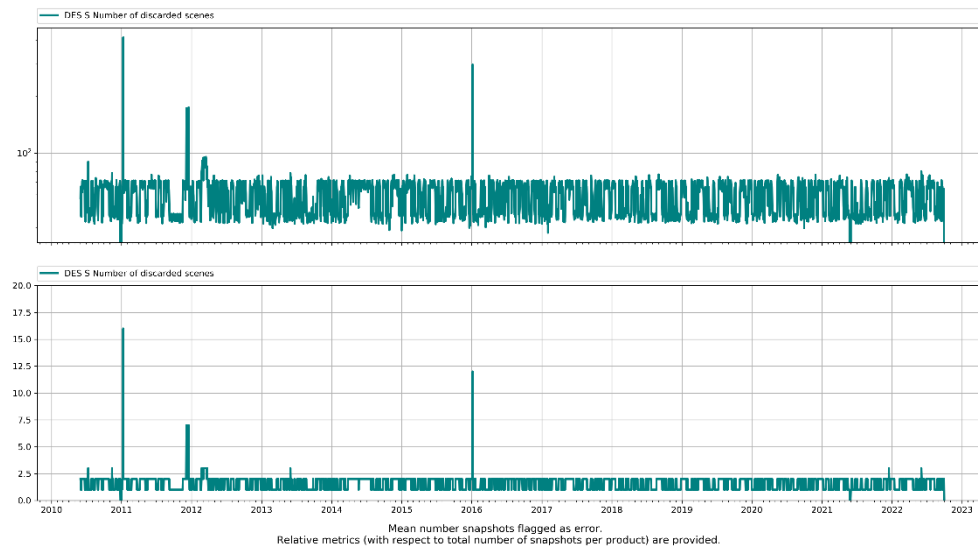


Figure 59: L1C V724 Discarded Scenes Descending Orbits

The number of discarded scenes counts the number of snapshots discarded at all the processing stages (L0, L1A, L1B and L1C). A snapshot may be discarded due to different reasons (see [RD1](#) for more comprehensive detailed description). The number of discards remain consistent (around 60 snapshots, < 2.5%) outside the commissioning period and the Jan 2011 anomaly. Nevertheless, two events with higher number of discards have been identified, at Dec 2011 and Jan 2016, respectively:

Between 20111213T173338 and 20111219T002236, 160-170 discards are reported per product.

For two products large discards are reported,
SM_REPR_MIR_SCSF1C_20160106T031835_20160106T033333_724_201_1 with 2868

snapshots discarded, and
SM_REPR_MIR_SCSF1C_20160106T042338_20160106T050151_724_200_1 with 1184

No clear cause for this has been found yet.

5.6 L2OS Ocean Target Transformation (OTT) Orchestration Analysis

The OTT correction is used by the L2OS processor for sea surface salinity retrieval. The correction is computed roughly on a daily basis by accumulating previous SMOS L1C measurements. The proper usage of the OTT correction is monitored, and results are present in **Figure 60** since June 2010. **Figure 60** shows the OTT delay defined as the delta time between the L2OS science product sensing time and the OTT correction validity time and averaged over 1 day period. As the validity time of the OTT correction depends on the dataset used to compute the correction, this OTT delay represents a quality indicator for the selection of the best OTT correction (i.e., the better correction is achieved by using an OTT with validity time closer to the L2OS sensing time).

Nominal OTT delay interval goes from 4 to 8 days of delay. Most of the OTT delays fall in the middle of such values, 5-6 days. OTT delays outside the nominal interval reveals anomalies either in the data selection policy or problems in accumulating L1C dataset (i.e., gaps or data rejection due to bad quality or presence of RFI).

For the current SMOS L2OS v700 dataset, the next anomaly periods affecting the OTT delay (i.e., delay above 8 days) have been found:

- 1) From 21/12/2010 to 08/01/2011: Electrical Stability Test and Temperature Reading anomalies with consequent unavailability of L1C data and increased OTT delay
- 2) From 01/04/2014 to 08/04/2014 OTT delays above 8 days due to L1C rejected data for OTT correction. Data rejection was due to corrupted L1C measurement affected by RFI.

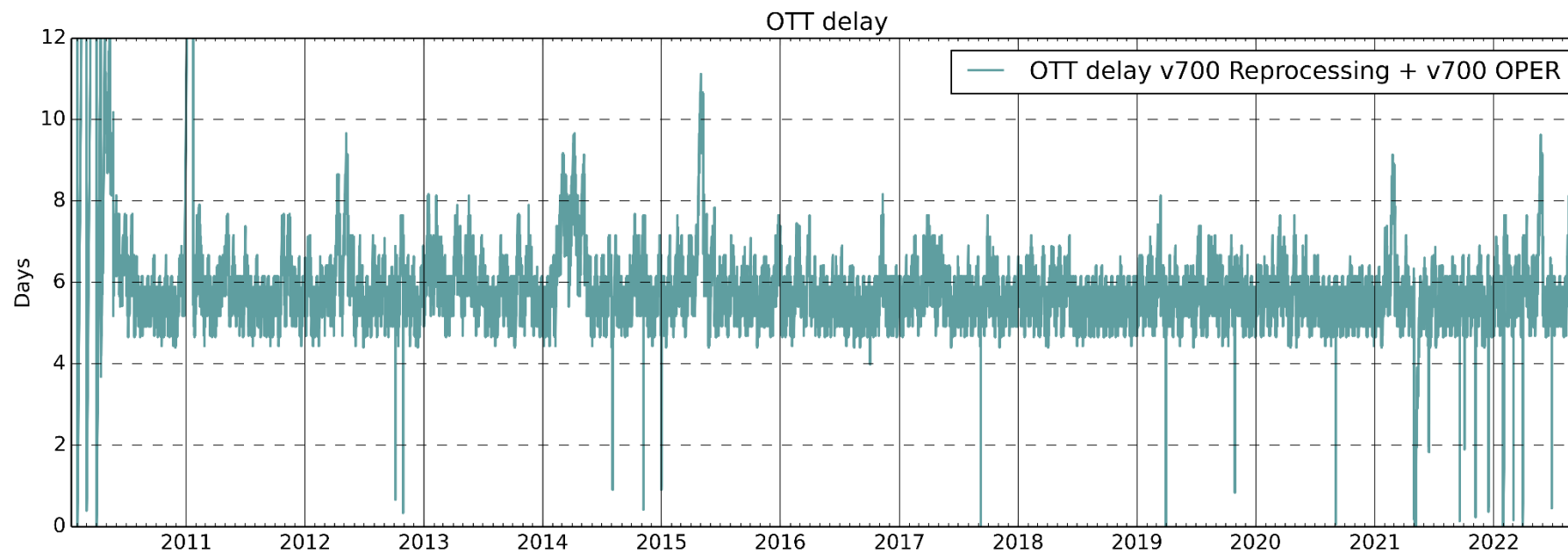


Figure 60: OTT delay per semi-orbit (Delta time between each L2OS product start time and the OTT correction validity start time file).

5.7 L2OS Retrievals Assessment

Analysis on the overall quality of the L2OS dataset is based on the evolution of the number of 'good quality' retrievals as shown in RD1 (ascending orbits) and in Figure 62 (descending orbits) as reported in the product header.

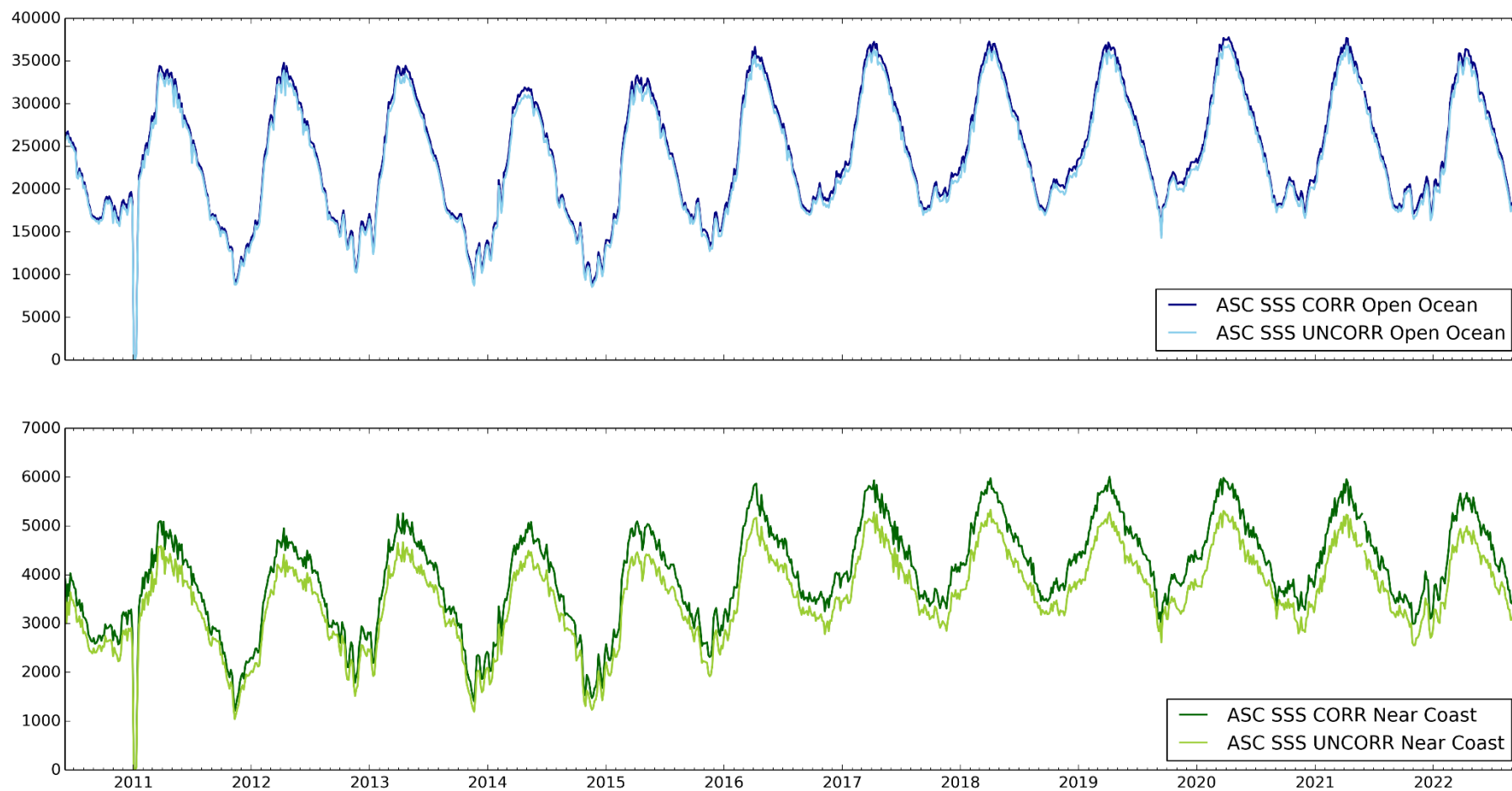
These 'Good Quality' retrievals are considered for two different areas: Open Ocean (more than 800km away from coastline) and Near Coast (within 800 km from the coastline).

Also, retrievals have been computed for the land-sea contamination corrected and uncorrected Sea Surface Salinity (SSS_corr, SSS_uncorr) and averaged daily, providing an estimation of the average number of retrievals per product. The seasonal variation in the number of good retrievals is mainly due to the criteria used to classify the data. This criteria is based on the following flags contained in the product:

- fg_ctrl_many_outliers
- fg_ctrl_sunglint
- fg_ctrl_moonglint
- fg_ctrl_gal_noise
- fg_ctrl_num_meas_low
- fg_sc_suspect_ice
- fg_sc_rain
- fg_sc_TEC_gradient

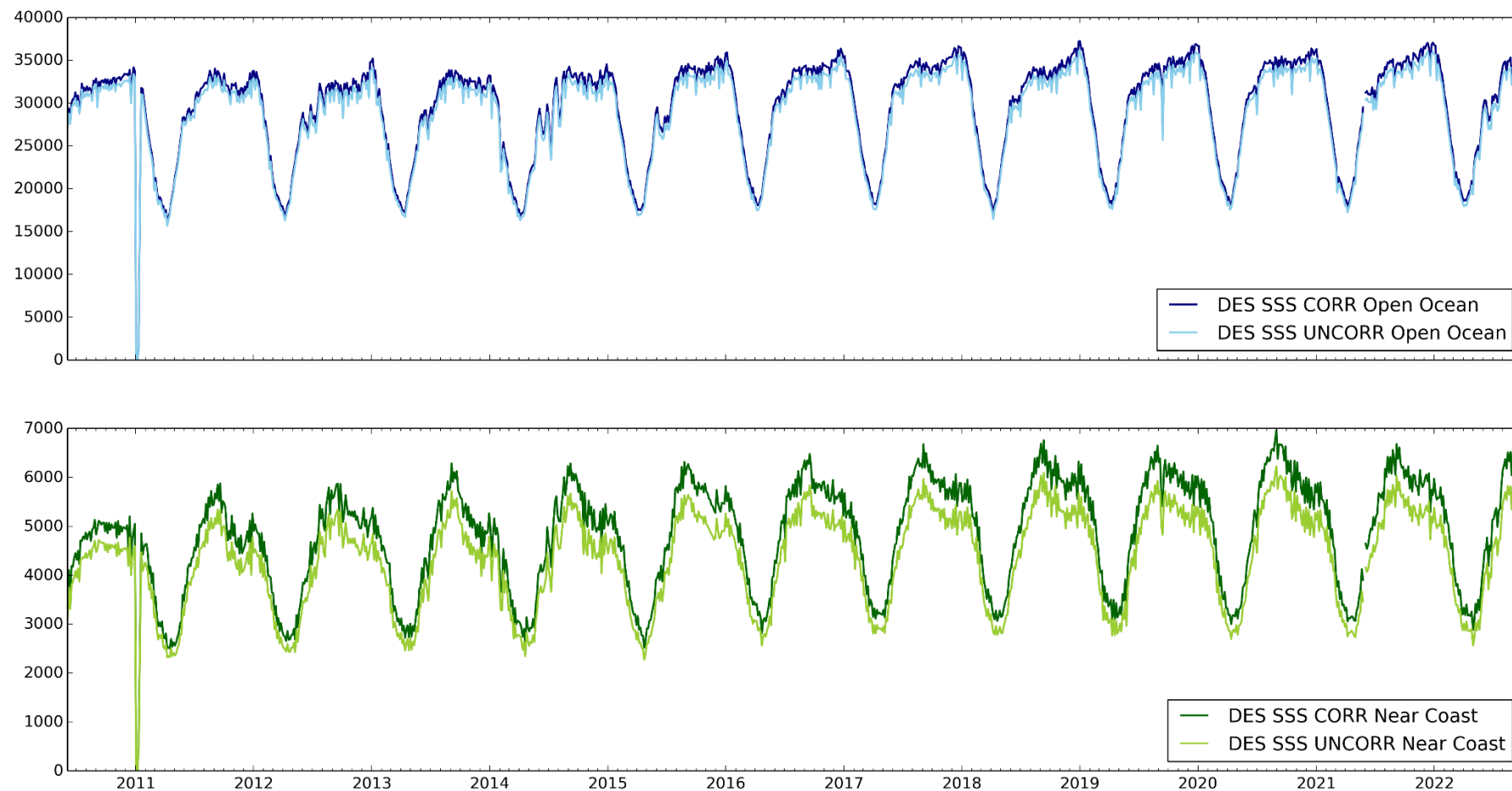
This criteria, will be reviewed in the next version of the L2OS processor and aligned with the "good quality" criteria recommended by the Expert Support Laboratory based on the following flags contained in the product:

- fg_ctrl_range
- fg_ctrl_sigma
- fg_ctrl_chi2
- fg_ctrl_chi2_P
- fg_ctrl_marq
- fg_ctrl_reach_maxiter



Number of successful salinity retrievals per retrieval case (Open Ocean and Near Coast). Computed as 4-day per product average.

Figure 61 ASC Open Ocean and Near Coast L2OS Good Quality Retrievals



Number of successful salinity retrievals per retrieval case (Open Ocean and Near Coast). Computed as 4-day per product average.

Figure 62 ASC Open Ocean and Near Coast L2OS Good Quality Retrievals

5.8 L2SM Retrievals Assessment

Analysis on the overall quality of the L2SM v700 dataset is based in the number of successful retrievals annotated in the SMUDP2 header file.

Such parameter is extracted for each retrieval branch. For some of the retrieval branches (i.e., Soil and Forest cover) this means a successful Soil Moisture retrieval. For the rest of branches, however, the parameter retrieved could be surface dielectric constant, optical depth, surface roughness or surface temperature. Please, refer to L2SM processor product specification for more details at this respect.

The metric is aggregated every 4 days in order to remove rapid variations originated due to geophysical changes in the surface. Also, it is provided as an average value per product, both in absolute value and in percentage with respect the total retrievals per branch. The metric is computed separately between ASC and DES semi-orbits, as the time of the overpass is different (ascending pass equator crossing at 06.00UTC a.m., descending pass equator crossing at 06.00UTC p.m.).

An increase on the number of retrievals for the 3 first years of operations is apparent. The origin of this is the reduction of RFI sources as a consequence of reporting the RFI case to the Spectrum Management Authorities since launch. In addition, v700 shows a higher number of retrievals with respect to v700. This is expected due to the change in the land cover auxiliary information especially relevant for Forest cover, but it is also apparent for other retrieval branches (e.g., Soil).

The relative total number of successfully retrievals presents some seasonal behaviour specially for descending semi-orbits. For some of the parameters (i.e., Forest, Snow) this bearing is especially clear for both ascending and descending and may be related with surface changes across the seasons.

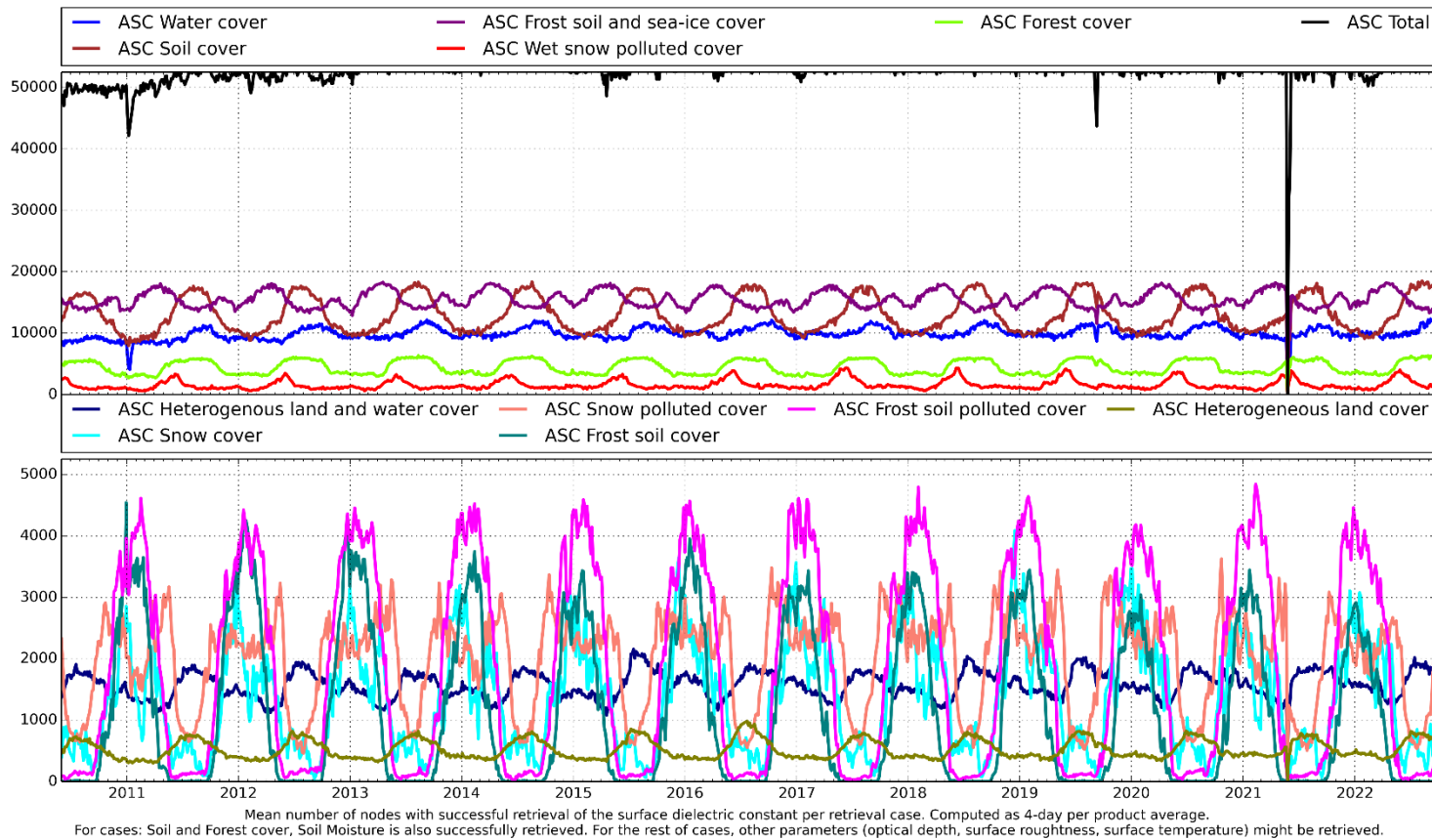


Figure 63: L2SM v700 Mean Retrievals Absolute - ASC

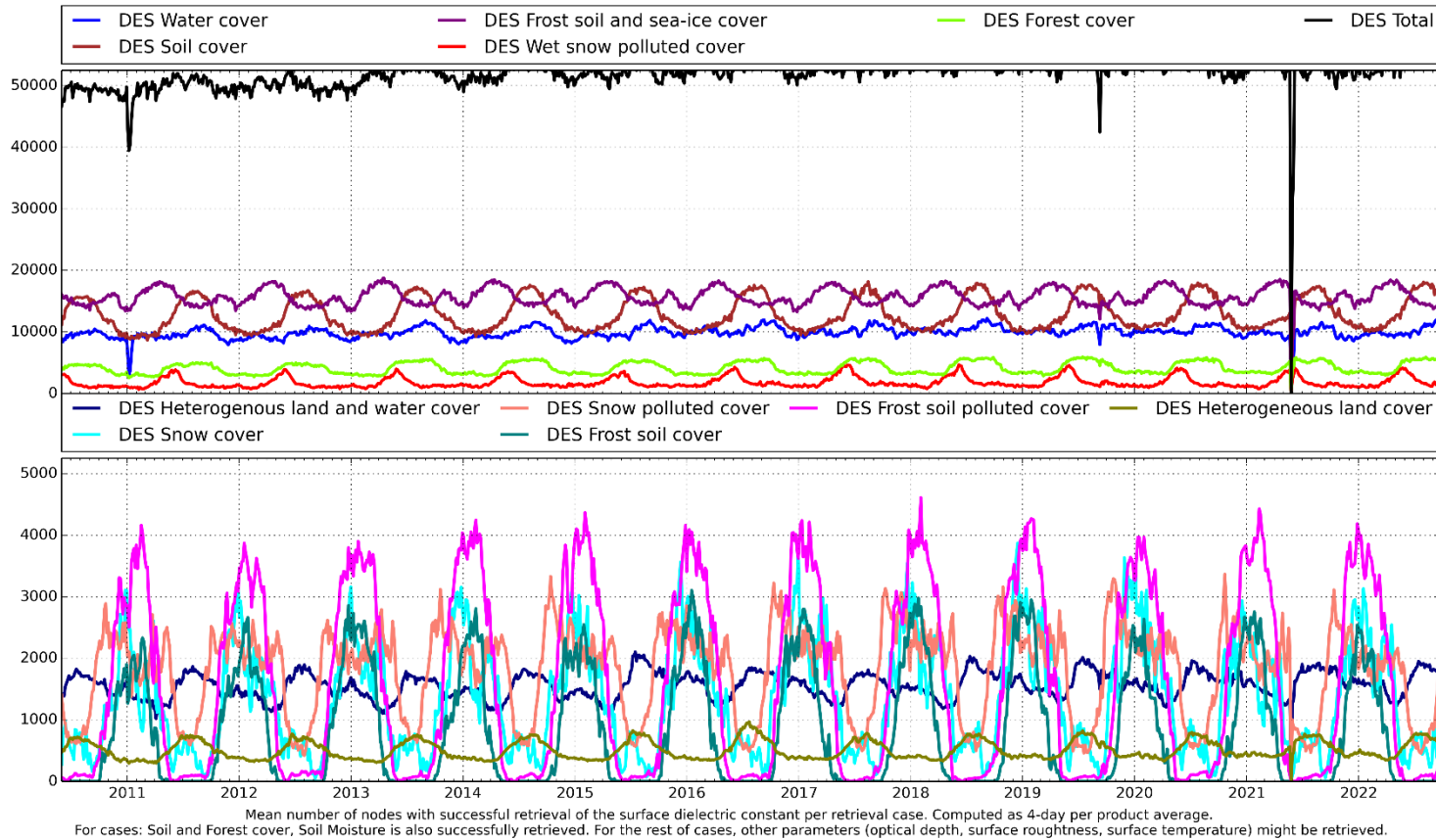


Figure 64: L2SM v700 Mean Retrievals Absolute - DES

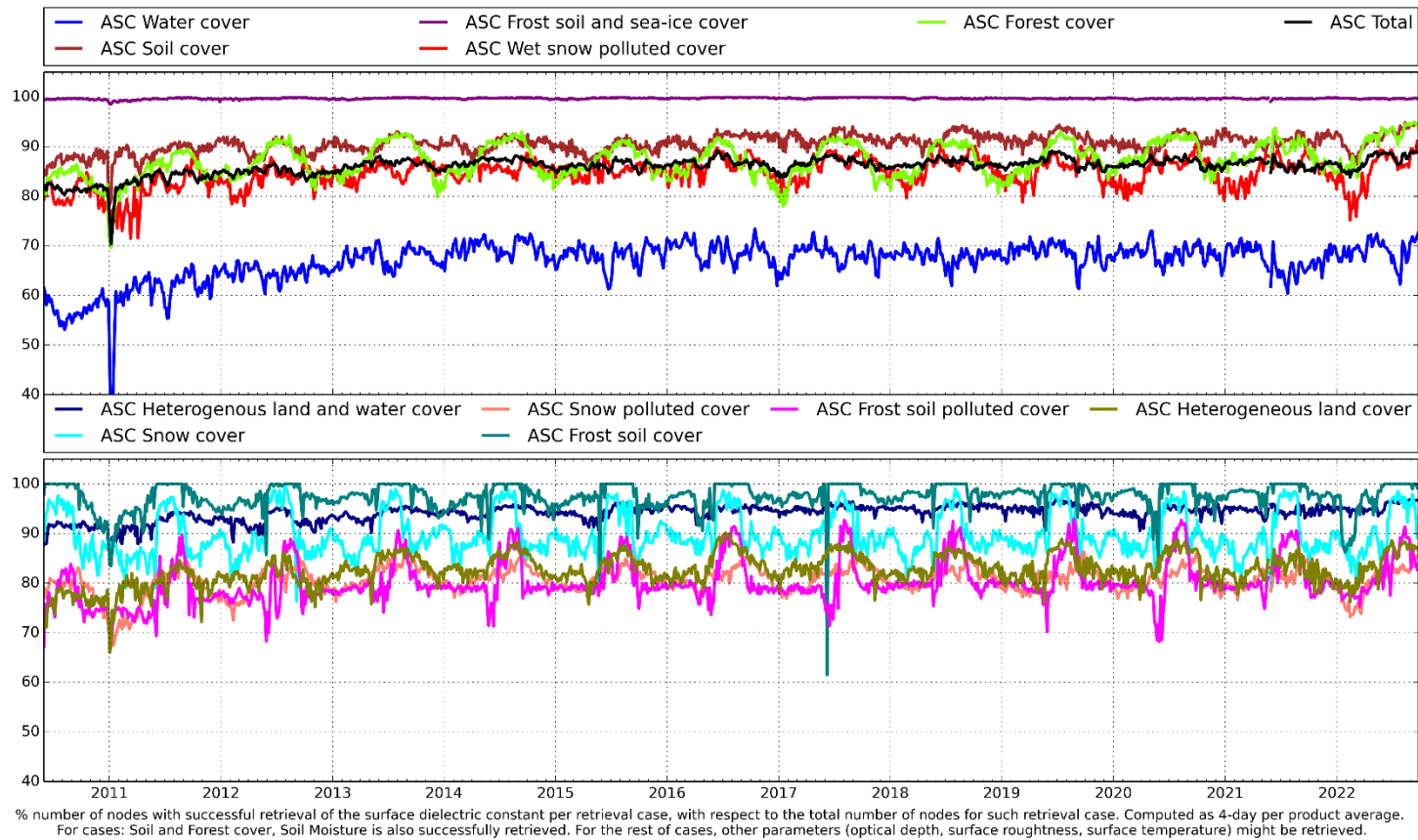


Figure 65: L2SM v700 Mean Retrievals Relative - ASC

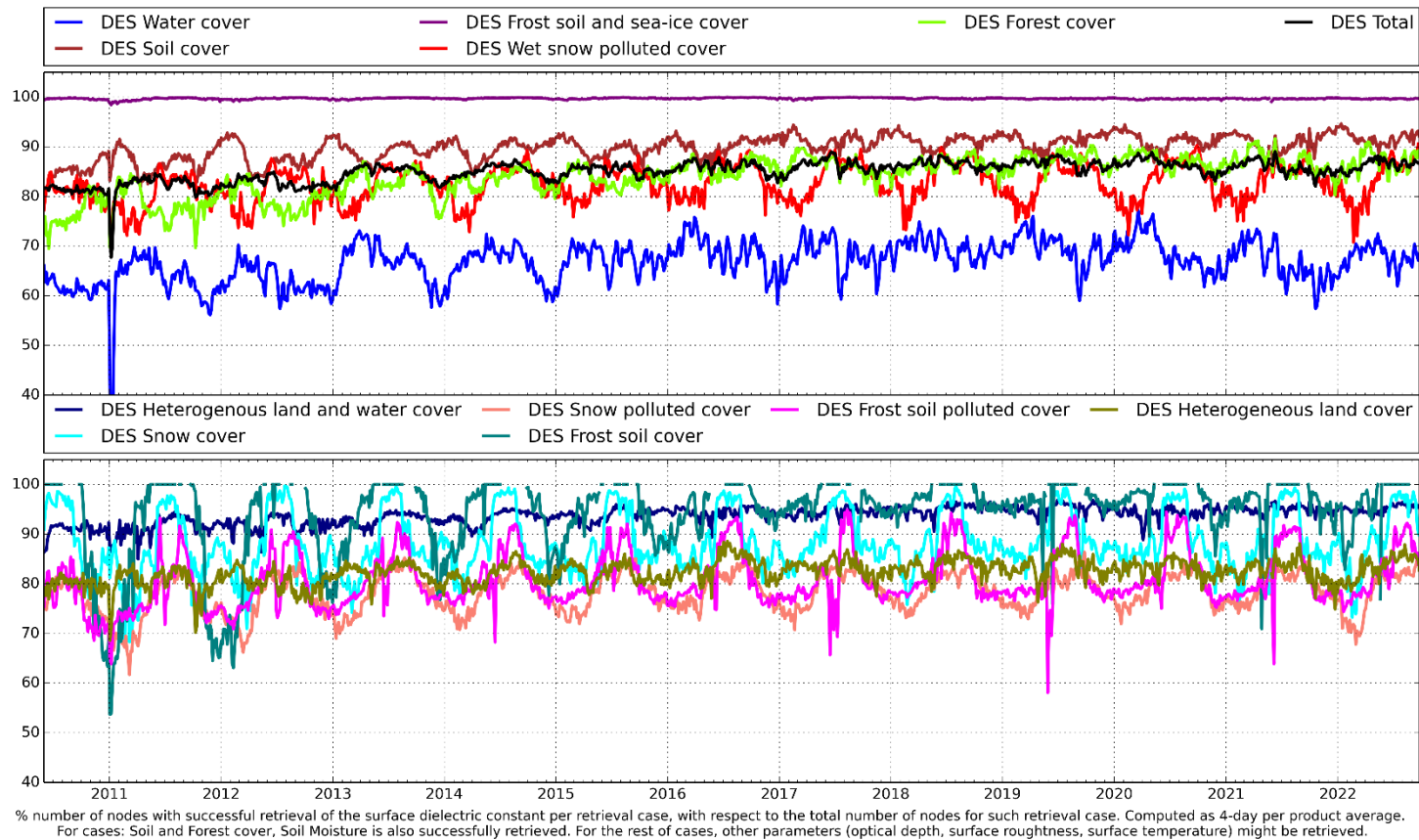


Figure 66: L2SM v700 Mean Retrievals Relative - DES

5.9 Pi-MEP: SSS Time series with Argo Buoy.

This section presents the systematic analysis of the Sea Surface Salinity difference between SMOS Level 2 measurements and in-situ (Argo buoys) measurements, specifically the time series of the monthly median and standard deviation of them from the SMOS Pi-MEP. For more information about the match-up database used to derive the differences please see the full monthly report from the SMOS Pilot-Mission Exploitation Platform for SSS available here (https://pimep.ifremer.fr/diffusion/smos-l2-v700_monthly-update/).

SMOS Pi-MEP is a project funded by ESA focused on validation of various satellite derived SSS products. The project gathers together European expertise groups (IFREMER, OceanDataLab, OceanScope) as well as NASA Expert Laboratories. For more detail on the project, please visit the [SMOS Pilot-Mission Exploitation Platform \(Pi-MEP\)](#).

Ascending and Descending Orbits.

For Figure 67:

- The *top panel* shows the time series of the monthly median SSS estimated over the full Global Ocean Pi-MEP region for both SMOS SSS L2 v700 satellite SSS product (in black) and the Argo in situ dataset (in blue) at the collected Pi-MEP match-up pairs.
- The *middle panel* shows the time series of the monthly median of Δ SSS (Satellite - Argo) for the collected Pi-MEP match-up pairs and estimated over the full Global Ocean Pi-MEP region.
- The *bottom panel* shows the time series of the monthly standard deviation of the Δ SSS (Satellite - Argo) for the collected Pi-MEP match-up pairs and estimated over the full Global Ocean Pi-MEP region.

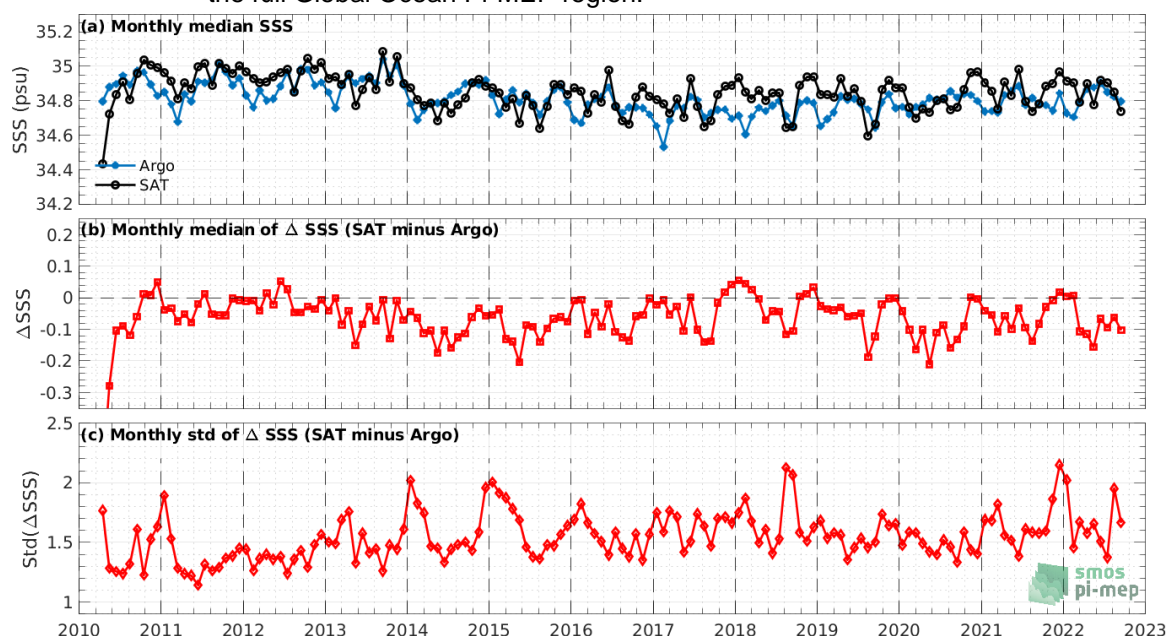


Figure 67 - Time series of the monthly median SSS (top), median of Δ SSS (Satellite - Argo) and Std of Δ SSS (Satellite - Argo) over the Global Ocean Pi-MEP region considering all match-ups collected by the Pi-MEP.

Ascending Orbits

For Figure 68:

- The *top panel* shows the time series of the monthly median SSS estimated over the full Global Ocean Pi-MEP region for both SMOS SSS L2 v700 satellite SSS product (in black) and the Argo in situ dataset (in blue) at the collected Pi-MEP match-up pairs.
- The *middle panel* shows the time series of the monthly median of Δ SSS (Satellite - Argo) for the collected Pi-MEP match-up pairs and estimated over the full Global Ocean Pi-MEP region.
- The *bottom panel* shows the time series of the monthly standard deviation of the Δ SSS (Satellite - Argo) for the collected Pi-MEP match-up pairs and estimated over the full Global Ocean Pi-MEP region.

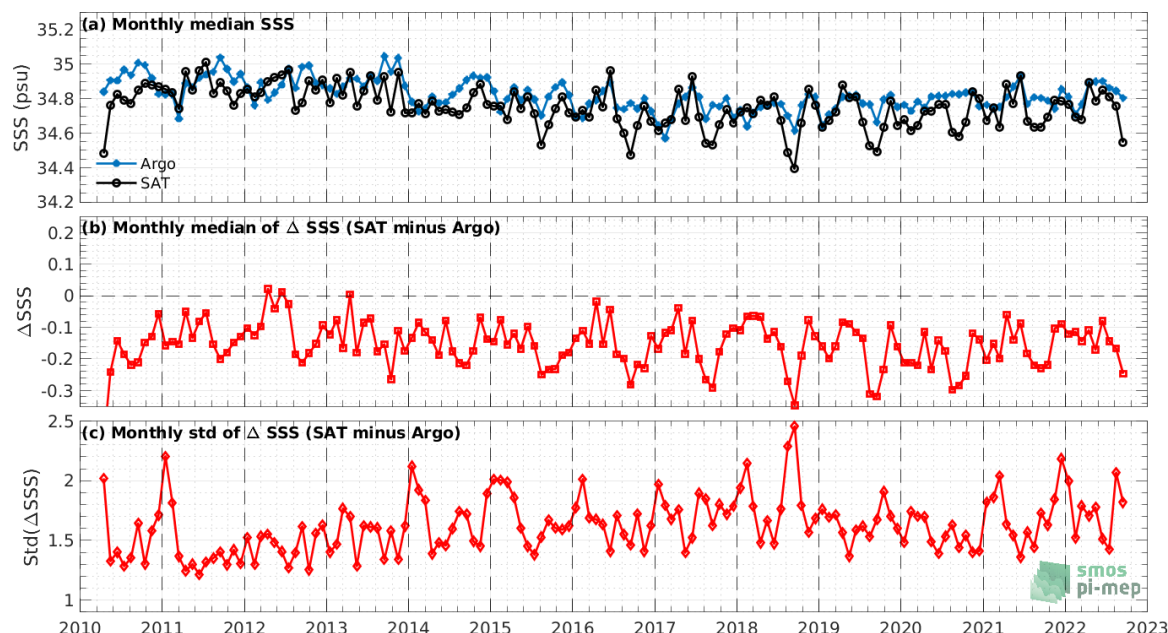


Figure 68 - Time series of the monthly median SSS (top), median of Δ SSS (Satellite - Argo) and Std of Δ SSS (Satellite - Argo) over the Global Ocean Pi-MEP region considering only ascending orbits from all match-ups collected by the Pi-MEP.

Descending Orbits

For Figure 69:

- The *top panel* shows the time series of the monthly median SSS estimated over the full Global Ocean Pi-MEP region for both SMOS SSS L2 v700 satellite SSS product (in black) and the Argo in situ dataset (in blue) at the collected Pi-MEP match-up pairs.

- The *middle panel* shows the time series of the monthly median of ΔSSS (Satellite - Argo) for the collected Pi-MEP match-up pairs and estimated over the full Global Ocean Pi-MEP region.
- The *bottom panel* shows the time series of the monthly standard deviation of the ΔSSS (Satellite - Argo) for the collected Pi-MEP match-up pairs and estimated over the full Global Ocean Pi-MEP region.

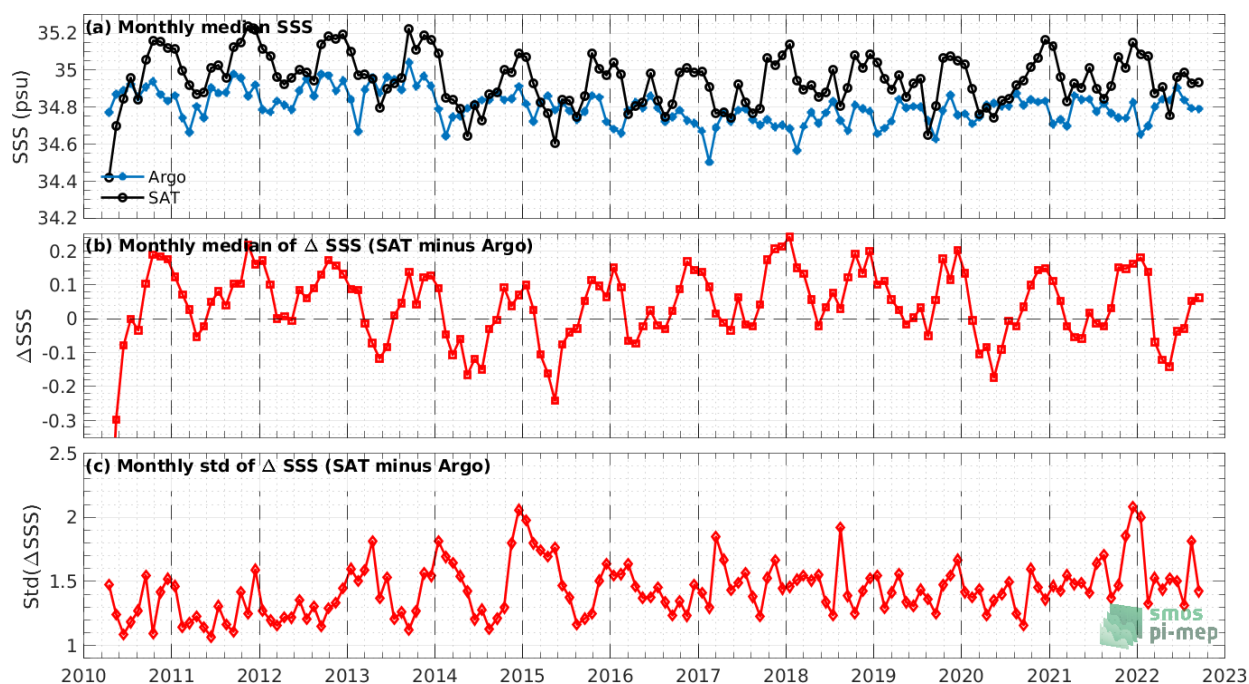


Figure 69 - Time series of the monthly median SSS (top), median of ΔSSS (Satellite - Argo) and Std of ΔSSS (Satellite - Argo) over the Global Ocean Pi-MEP region considering only descending orbits from all match-ups collected by the Pi-MEP.

6 PRODUCT QUALITY ANALYSIS

Level 1 data quality for September has found to be nominal except in the time intervals listed in the section 4.5. Weekly maps for ascending and descending passes for the Stokes 1, Stokes 3 and Stokes 4 in videos format can be found at: <https://earth.esa.int/eogateway/instruments/miras/quality-control-reports/smos-videos>

All the artificial patterns in the maps can be explained by the presence of RFIs.

Level 2 Soil Moisture data quality for September has found to be nominal. Weekly maps for ascending and descending passes for the soil moisture in video format can be found at: <https://earth.esa.int/eogateway/instruments/miras/quality-control-reports/smos-videos>

Level 2 Sea Surface Salinity data quality is nominal in the reporting period. Weekly maps for ascending and descending passes for good quality retrieved sea surface salinity in video format can be found at: <https://earth.esa.int/eogateway/instruments/miras/quality-control-reports/smos-videos>

The lack of good retrieval at descending passes during the boreal winter season is less evident for winter season 2015/2016, 2016/2017 and 2017/2018, This fact points out that thermal effect on the instrument due to eclipse is only one contributor and other sources (e.g., L-band Sun signal direct or reflected) impacting the number of good retrievals are under investigation by the calibration team and Level 2 ESL.

For more details on soil moisture and sea surface salinity retrieval algorithms and caveats in data usage see the **Level 2 Algorithm Theoretical Baseline Documents** and the read-me-first note available here:

- **L2OS:** <https://earth.esa.int/eogateway/documents/20142/37627/SMOS-L2OS-ATBD.pdf?text=smos+atdb>
- **L2SM:** <https://earth.esa.int/eogateway/documents/20142/37627/SMOS-L2-SM-ATBD.pdf?text=smos+atdb>

7 ADF CONFIGURATION AT THE END OF THE REPORTING PERIOD

ADF File Type	Operational ADF Version (DPGS Baseline)	Updated
AUX_APDL	SM_OPER_AUX_APDL_20050101T000000_20500101T000000_300_004_3.EEF	No
AUX_APDNRT	SM_OPER_AUX_APDNRT_20050101T000000_20500101T000000_208_001_6.EEF	No
AUX_APDS	SM_OPER_AUX_APDS_20050101T000000_20500101T000000_300_004_3.EEF	No
AUX_ATMOS	SM_OPER_AUX_ATMOS_20050101T000000_20500101T000000_001_010_3.EEF	No
AUX_BFP	SM_OPER_AUX_BFP_20050101T000000_20500101T000000_340_004_3.EEF	No
AUX_BNDLST	SM_OPER_AUX_BNDLST_20050101T000000_20160308T000000_303_004_3 SM_OPER_AUX_BNDLST_20160308T000000_20500101T000000_303_004_3 SM_OPER_AUX_BNDLST_20190305T000000_20500101T000000_303_004_3	No
AUX_BSCAT	SM_OPER_AUX_BSCAT_20050101T000000_20500101T000000_300_003_3	No
AUX_BULL_B	SM_OPER_AUX_BULL_B_20220702T000000_20500101T000000_120_001_3	Yes
AUX_BWGHT	SM_OPER_AUX_BWGHT_20050101T000000_20500101T000000_340_006_3.EEF	No
AUX_CNFFAR	SM_OPER_AUX_CNFFAR_20050101T000000_20500101T000000_100_002_3.EEF	No
AUX_CNFL0P	SM_OPER_AUX_CNFL0P_20050101T000000_20500101T000000_001_007_3.EEF	No
AUX_CNFL1P	SM_OPER_AUX_CNFL1P_20110206T010100_20500101T000000_721_055_3.EEF	No
AUX_CNFNRT	SM_OPER_AUX_CNFNRT_20050101T000000_20500101T000000_620_012_3.EEF	No
AUX_CNFOSD	SM_OPER_AUX_CNFOSD_20050101T000000_20500101T000000_001_029_3.EEF	No
AUX_CNFOSF	SM_OPER_AUX_CNFOSF_20050101T000000_20500101T000000_001_032_3.EEF	No
AUX_CNFSMD	SM_OPER_AUX_CNFSMD_20050101T000000_20500101T000000_001_017_3.EEF	No
AUX_CNFSMF	SM_OPER_AUX_CNFSMF_20050101T000000_20500101T000000_001_017_3.EEF	No
AUX_DFFFRA	SM_OPER_AUX_DFFFRA_20050101T000000_20500101T000000_001_007_3	No
AUX_DFFLAI	SM_OPER_AUX_DFFLAI_20220101T000000_20220111T014000_600_001_3 SM_OPER_AUX_DFFLAI_20220111T000000_20220121T014000_600_001_3 SM_OPER_AUX_DFFLAI_20220121T000000_20220203T014000_600_001_3 SM_OPER_AUX_DFFLAI_20220203T000000_20220213T014000_600_001_3 SM_OPER_AUX_DFFLAI_20220213T000000_20220223T014000_600_001_3 SM_OPER_AUX_DFFLAI_20220223T000000_20220302T014000_600_001_3 SM_OPER_AUX_DFFLAI_20220302T000000_20220312T014000_600_001_3 SM_OPER_AUX_DFFLAI_20220312T000000_20220322T014000_600_001_3 SM_OPER_AUX_DFFLAI_20220322T000000_20220402T014000_600_001_3 SM_OPER_AUX_DFFLAI_20220402T000000_20220412T014000_600_001_3 SM_OPER_AUX_DFFLAI_20220412T000000_20220422T014000_600_001_3 SM_OPER_AUX_DFFLAI_20220422T000000_20220501T014000_600_001_3 SM_OPER_AUX_DFFLAI_20220501T000000_20220511T014000_600_001_3 SM_OPER_AUX_DFFLAI_20220511T000000_20220521T014000_600_001_3 SM_OPER_AUX_DFFLAI_20220521T000000_20220601T014000_600_001_3 SM_OPER_AUX_DFFLAI_20220601T000000_20220611T014000_600_001_3 SM_OPER_AUX_DFFLAI_20220611T000000_20220621T014000_600_001_3 SM_OPER_AUX_DFFLAI_20220621T000000_20220630T014000_600_001_3 SM_OPER_AUX_DFFLAI_20220630T000000_20220710T014000_600_001_3 SM_OPER_AUX_DFFLAI_20220710T000000_20220720T014000_600_001_3 SM_OPER_AUX_DFFLAI_20220720T000000_20220730T014000_600_001_3 SM_OPER_AUX_DFFLAI_20220730T000000_20220809T014000_600_001_3 SM_OPER_AUX_DFFLAI_20220809T000000_20220819T014000_600_001_3 SM_OPER_AUX_DFFLAI_20220819T000000_20220829T014000_600_001_3 SM_OPER_AUX_DFFLAI_20220829T000000_20220909T014000_600_001_3 SM_OPER_AUX_DFFLAI_20220909T000000_20220919T014000_600_001_3 SM_OPER_AUX_DFFLAI_20220919T000000_20220929T014000_600_001_3 SM_OPER_AUX_DFFLAI_20220929T000000_20221008T014000_600_001_3 SM_OPER_AUX_DFFLAI_20221008T000000_20221018T014000_600_001_3 SM_OPER_AUX_DFFLAI_20221018T000000_20221028T014000_600_001_3 SM_OPER_AUX_DFFLAI_20221028T000000_20221108T014000_600_001_3 SM_OPER_AUX_DFFLAI_20221108T000000_20221118T014000_600_001_3 SM_OPER_AUX_DFFLAI_20221118T000000_20221128T014000_600_001_3 SM_OPER_AUX_DFFLAI_20221128T000000_20221207T014000_600_001_3 SM_OPER_AUX_DFFLAI_20221207T000000_20221217T014000_600_001_3 SM_OPER_AUX_DFFLAI_20221217T000000_20230101T014000_600_001_3	No
AUX_DFFLMX	SM_OPER_AUX_DFFLMX_20050101T000000_20500101T000000_001_006_3	No
AUX_DFFSOI	SM_OPER_AUX_DFFSOI_20050101T000000_20500101T000000_001_003_3	No
AUX_DFFXYZ	SM_OPER_AUX_DFFXYZ_20050101T000000_20500101T000000_001_003_3	No

AUX_DGG	SM_OPER_AUX_DGG_20050101T000000_20500101T000000_300_003_3	No
AUX_DGGXYZ	SM_OPER_AUX_DGGXYZ_20050101T000000_20500101T000000_001_004_3	No
AUX_DISTAN	SM_OPER_AUX_DISTAN_20050101T000000_20500101T000000_001_011_3	No
AUX_DTBCUR	SM_REPR_AUX_DTBCUR_20210520T083700_20500101T000000_699_320_1 Initialization file for the deployment of the L2OS V700 processor.	No
AUX_ECOLAI	SM_OPER_AUX_ECOLAI_20050101T000000_20500101T000000_305_006_3	No
AUX_ECMCDF	SM_OPER_AUX_ECMCDF_20101109T000000_20500101T000000_001_003_3.EEF SM_OPER_AUX_ECMCDF_20050101T000000_20101109T000000_001_003_3	No
AUX_FAIL	SM_OPER_AUX_FAIL_20050101T000000_20500101T000000_300_004_3.EEF	No
AUX_FLTSEA	SM_OPER_AUX_FLTSEA_20050101T000000_20500101T000000_001_012_3.EEF	No
AUX_FOAM	SM_OPER_AUX_FOAM_20050101T000000_20500101T000000_001_011_3	No
AUX_FRSNEL	SM_OPER_AUX_FRSNEL_20050101T000000_20500101T000000_720_001_3	No
AUX_GAL_OS	SM_OPER_AUX_GAL_OS_20050101T000000_20500101T000000_001_011_3	No
AUX_GAL_SM	SM_OPER_AUX_GAL_SM_20050101T000000_20500101T000000_001_003_3	No
AUX_GAL2OS	SM_OPER_AUX_GAL2OS_20050101T000000_20500101T000000_001_016_3	No
AUX_GALAXY	SM_OPER_AUX_GALAXY_20050101T000000_20500101T000000_300_004_3	No
AUX_GALNIR	SM_OPER_AUX_GALNIR_20050101T000000_20500101T000000_300_003_3	No
AUX_LANDCL	SM_OPER_AUX_LANDCL_20050101T000000_20500101T000000_001_006_3.EEF	No
AUX_LCF	SM_OPER_AUX_LCF_20050101T000000_20500101T000000_720_019_3.EEF	No
AUX_LSMASK	Discontinued (dynamic ADF for V7xx baseline onwards)	No
AUX_MASK	SM_OPER_AUX_MASK_20050101T000000_20500101T000000_300_002_3	No
AUX_MISP	SM_OPER_AUX_MISP_20050101T000000_20500101T000000_300_004_3.EEF	No
AUX_MN_WEF	SM_OPER_AUX_MN_WEF_20050101T000000_20500101T000000_001_002_3	No
AUX_MOONT	SM_OPER_AUX_MOONT_20050101T000000_20500101T000000_300_002_3	No
AUX_MSOTT	SM_OPER_AUX_MSOTT_20050101T000000_20500101T000000_001_002_3	No
AUX_N256	SM_OPER_AUX_N256_20050101T000000_20500101T000000_504_002_3	No
AUX_NIR	SM_OPER_AUX_NIR_20050101T000000_20500101T000000_720_012_3.EEF	No
AUX_NRTMSK	SM_OPER_AUX_NRTMSK_20050101T000000_20500101T000000_207_001_6	No
AUX_OTT1D	SM_REPR_AUX_OTT1D_20210520T083700_20500101T000000_699_320_1 Initialization file for the deployment of the L2OS V700 processor. Since level 2 OS processor V62x the new file is generated on routine basis by the level 2 post processor	No
AUX_OTT1F	SM_REPR_AUX_OTT1F_20210520T083700_20500101T000000_699_320_1 Initialization file for the deployment of the L2OS V700 processor. Since level 2 OS processor V62x the new file is generated on routine basis by the level 2 post processor	No
AUX_OTT2D	SM_REPR_AUX_OTT2D_20210520T083700_20500101T000000_699_320_1 Initialization file for the deployment of the L2OS V700 processor. Since level 2 OS processor V62x the new file is generated on routine basis by the level 2 post processor	No
AUX_OTT2F	SM_REPR_AUX_OTT2F_20210520T083700_20500101T000000_699_320_1 Initialization file for the deployment of the L2OS V700 processor. Since level 2 OS processor V62x the new file is generated on routine basis by the level 2 post processor	No
AUX_OTT3D	SM_REPR_AUX_OTT3D_20210520T083700_20500101T000000_699_320_1 Initialization file for the deployment of the L2OS V700 processor. Since level 2 OS processor V62x the new file is generated on routine basis by the level 2 post processor	No
AUX_OTT3F	SM_REPR_AUX_OTT3F_20210520T083700_20500101T000000_699_320_1 Initialization file for the deployment of the L2OS V700 processor. Since level 2 OS processor V62x the new file is generated on routine basis by the level 2 post processor	No
AUX_PATT	SM_OPER_AUX_PATT_20050101T000000_20500101T000000_720_004_3	No
AUX_PLM	SM_OPER_AUX_PLM_20050101T000000_20500101T000000_600_008_3.EEF	No

AUX_PMS__	SM_OPER_AUX_PMS__20050101T000000_20500101T000000_711_013_3.EEF	No
AUX_RFI__	SM_OPER_AUX_RFI__20050101T000000_20500101T000000_300_003_3	No
AUX_RFILST	Since level 1 processor version V62x the file is generated by CATDS on monthly basis	No
AUX_RGHNS1	SM_OPER_AUX_RGHNS1_20050101T000000_20500101T000000_001_016_3	No
AUX_RGHNS2	SM_OPER_AUX_RGHNS2_20050101T000000_20500101T000000_001_013_3	No
AUX_RGHNS3	SM_OPER_AUX_RGHNS3_20050101T000000_20500101T000000_001_016_3	No
AUX_SGLINT	SM_OPER_AUX_SGLINT_20050101T000000_20500101T000000_001_012_3	No
AUX_SOIL_P	Discontinued (replaced by AUX_DFFSOI for V6xx baseline onwards)	No
AUX_SPAR__	SM_OPER_AUX_SPAR__20110112T091500_20500101T000000_720_013_3.EEF	No
	SM_OPER_AUX_SPAR__20100111T120700_20110112T091500_720_013_3.EEF	
	SM_OPER_AUX_SPAR__20050101T000000_20100111T120700_720_013_3.EEF	
AUX_SSS__	SM_OPER_AUX_SSS__20050101T000000_20500101T000000_001_014_3	No
AUX_SSSCLI	SM_OPER_AUX_SSSCLI_20050101T000000_20500101T000000_001_002_3	No
AUX_SUNT__	SM_OPER_AUX_SUNT__20050101T000000_20500101T000000_300_002_3	No
AUX_WEF__	SM_OPER_AUX_WEF__20050101T000000_20500101T000000_001_003_3	No
MPL_ORBSCT	SM_OPER_MPL_ORBSCT_20091102T031142_20500101T000000_464_001.EEF	Yes

8 APPENDIX A. CONFIGURATION DOCUMENT LIST

The list of internal documents used for the generation of this report is:

- Unavailability.xls
- Details_Calibrations.xls
- SMOS-CEC-VEG-IPF-REP-0609_v3.01_SMOS_Auxiliary_Data_File_List_202200929_signed.pdf

This Page Is Intentionally Blank

End of Document